This is a repository copy of *The Brampton kame belt and Pennine escarpment meltwater channel system (Cumbria, UK): morphology, sedimentology and formation*.

The Brampton Kame Belt and Pennine Escarpment meltwater channel system (Cumbria, UK): Morphology, Sedimentology and Formation

Stephen J. Livingstone, David J. A. Evans, Colm Ó Cofaigh, Jonathon Hopkins

Abstract

The Brampton kame belt represents one the largest glaciofluvial complexes within the UK. It is composed of an array of landform and sediment assemblages, associated with a suite of meltwater channels and situated within a palimpsest landscape of glacial features in the heart of the most dynamic part of the British-Irish ice sheet. Glacial geomorphological mapping and sedimentological analysis has allowed a detailed reconstruction of both the morphological features and the temporal evolution of the Brampton kame belt, with processes informed by modern analogues from modern ice margins. The kame belt demonstrates the development of a complex glacier karst typified by the evolution of subglacial meltwater tunnels into an englacial and supraglacial meltwater system dominated by ice-walled lakes and migrating ice-contact drainage networks. Topographic inversion led to the extensive re-working of sediments, with vertical collapse (associated with the melt-out of dead ice) and debris flows causing partial disintegration of the morphology. The resultant landform comprises a series of kettle holes, discontinuous ridges (eskers) and flat-topped hills (ice-walled lake plains). The Pennine escarpment meltwater network, which fed the Brampton kame belt, is composed of an anastomosing subglacial channel system and flights of lateral channels. Water was transferred into the subglacial system via a series of subglacial chutes during changes in the basal ice thermal regime. The Brampton kame belt is envisaged to have formed during the stagnation of ice in the lee of the Pennines and Penrith sandstone outcrop as ice retreated westwards across the Tyne Gap into the Solway Lowlands. The formation of the Brampton kame belt also has particular conceptual resonance in terms of constraining the nature of kame genesis, whereby an evolving glacier karst is a key mechanism in the spatial and temporal development of ice contact sediment-landform associations.

Introduction

Kames constitute some of the most diverse and complex landform and sediment assemblages in glaciated landscapes. Their morphology often comprises an array of ridges, flat-topped hills and depressions which contain a diverse range of glaciofluvial and glaciolacustrine sediments (e.g. Holmes, 1947; Price, 1969, 1973; Paul, 1983; Thomas *et al.*, 1985; Benn & Evans, 1998; Evans & Twigg, 2002; Evans *et al*). Consequently the site-specific interpretation of these landforms is often contentious (cf. Gravenor & Kupsch, 1959; Huddart & Bennett, 1997; Owen, 1997; Thomas & Montague, 1997; Johnson & Clayton, 2003). However, observations of glaciofluvial landform-sediment assemblages along modern glacier margins (e.g. Price, 1966, 1969, 1973; Huddart, *et*

al., 1999; Russell, *et al*. 2001, 2005, 2007; Evans & Twigg, 2002; Evans *et al*. In press) are proving increasingly useful in constraining the genesis of kames and their associations with ice contact fans and esker networks. In light of recent advances it is appropriate to re-appraise models of kame formation in Pleistocene environments. The "Brampton kame belt" in Cumbria (cf. Trotter, 1929; Trotter & Hollingworth 1932; Huddart, 1970, 1981) represents one of the largest assemblages of glaciofluvial material in the United Kingdom at over 44 km^2 (Livingstone *et al*., 2008). It represents a major depositional episode during the advanced stages of recession of the Late Devensian (Dimlington stadial) British and Irish Sea Sheet (BIIS) in the Solway Lowlands (Trotter, 1929; Huddart, 1970, 1981). Being able to elucidate the mode of formation of such a large feature, together with its genetic association with a complex suite of meltwater channels on the Pennine Escarpment (Fig. 1) to the south (Arthurton & Wadge 1981), is critical to reconstructing the style of deglaciation at the centre of the BIIS.

This paper has two aims: to determine the origin of the various components of the Brampton kame belt; and to use this information to constrain the nature, configuration and timing of deglaciation of the area comprising the Solway Lowlands, the Vale of Eden/Pennine Escarpment and westernmost Tyne Gap, the core region at the centre of the most dynamic part of the BIIS (Salt & Evans 2004; Livingstone *et al*. 2008; Evans *et al*. 2009).

Process-form models of kame production and previous work on the Brampton area

The term "kame" is used by glacial geomorphologists to refer to "steep-sided, variously shaped mounds composed chiefly of sand and gravel, formed by supra-glacial or ice-contact glacifluvial deposition" (Benn & Evans, 1998, *p487*). Kame topography forms a composite landscape consisting of flat-topped mounds, ridges and hollows (Fig. 2) that evolve when large quantities of sediment are reworked by englacial and supraglacial drainage networks during the final retreat of ice (Cook, 1946; Holmes 1947; Paul 1983). In general terms hollows are formed by the differential melting of debris-covered dead ice and the enlargement and collapse of tunnels during downwasting (Clayton 1964; Clayton & Cherry 1967; Krüger 1994). The deposition of glaciofluvial, glaciolacustrine and interfingering debris flow deposits in the hollows initiates continuous topographic inversion during ablation, forming positive relief features (Boulton 1967, 1972; Price 1965, 1969). The removal of supporting ice produces complex patterns of fault and fold structures within the kame deposits (Boulton 1972; McDonald & Shilts, 1975; Johnson & Clayton 2003).

Flat-topped mounds (kame plateaus) are the product of deposition in ice-walled lake plains (e.g. Smed 1962; Clayton & Cherry, 1967; Johnson & Clayton 2003; Clayton *et al*., 2008) or supraglacial ponds (e.g. Mager & Fitzsimons, 2007). Supraglacial ponds collect sequences of heavily disturbed stratified sediments and mass flow deposits which typically show evidence of water escape structures, soft sediment deposition, and cut and fill sequences (Eyles, 1979; Eyles *et al*., 1987; Mager & Fitzsimons, 2007). Ice-walled lake plains are characterised by flat-tops, rhythmically bedded fine-grained sediments and deltaic deposits. At the margins of the upstanding lake plains or plateaux these sediments are typically extensively faulted due to the removal of the supporting ice walls during melt-out (cf. Clayton *et al*., 2008).

Kame terraces are "gently sloping depositional terraces perched on valley sides…deposited by meltwater streams flowing between glacier margins and the adjacent valley wall" (Benn & Evans, 1998, *p. 490*). Thus a series of kame terraces can document the periodic retreat and surface lowering of a glacier (Sissons, 1958). Kame terraces typically exhibit pitted surfaces due to the melt out of buried ice. Substantial bodies of glacier ice may lie beneath the deposits of marginal streams (McKenzie 1969; Evans *et al*. In press) making it unlikely that the flat river bed will survive final melt-out, and will develop instead into an elongate chain of kame and kettle topography in which the kame mound summits appear accordant from a distance.

Kame topography often contains features whose form is dictated by the palaeo-drainage network or guidance of supraglacial streams by controlled moraine (*sensu* Evans 2009) produced by debris-charged folia rising to the glacier surface (e.g. Thomas *et al*. 1985). Consequently, discontinuous sinuous ridges composed of glaciofluvial sediments are visible amongst the kame and kettle terrain (e.g. Price, 1969; Twigg & Evans, 2002). These esker-like ridges often show a great deal of complexity (e.g. the "Carstairs kames" in Scotland; Huddart & Bennett, 1997; Thomas & Montague, 1997), necessitating multiple phases or mechanisms of construction. Glaciofluvial sediment can accumulate at various levels in a glacier and may evolve from a subglacial to an englacial and supraglacial assemblage during ice wastage (e.g. Huddart, *et al*. 1999).

The Brampton kame belt was first investigated by Trotter (1929) (Fig. 3). He proposed a model of ice frontal retreat, with ridges attributed to ice-contact outwash formed during stillstands. These were fed by eskers ["oses" in Trotter, 1929] which were interpreted as englacial conduits (Fig. 3). These complex esker deposits, often consisting of anastomising limbs, were attributed to the crevassed condition of the ice which produced multiple changes in stream course. Flat-topped hills marked ice-marginal delta fronts (Fig. 3), again fed from englacial streams, built up to lake level. The circular hollows were interpreted by Trotter as kettle holes formed by ablating dead ice. The kame belt was re-investigated by Huddart (1970) who attributed the landforms to supraglacial deposition during *in situ* ice stagnation, rather than the ice-marginal depo-centres envisaged by Trotter. The depositional ridges in the kame belt were interpreted by Huddart as the products of a rapidly shifting glaciofluvial drainage network following open crevasses. The network was fed from englacial or subglacial tunnels. The flat-topped hills were interpreted as standing bodies of water surrounded by stagnant ice (i.e. ice-walled lake plains).

The Brampton kame belt is contiguous with a series of meltwater channels and glaciofluvial deposits that extend southwards along the Pennine escarpment and northeastwards into the Tyne Gap (Fig. 3, 4) (Trotter, 1929; Arthurton & Wadge, 1981; Livingstone *et al*., 2008). The Hallbankgate esker, which emerges from the northern end of the kame belt, trends into an 8 km long meltwater channel cutting west to east across the Irthing-South Tyne watershed (Fig. 3) and feeding into the Tyne Valley system (Trotter, 1929; Livingstone *et al*., 2008). Another channel to the north of the Brampton kame belt at Gilsland cuts NW-SE across the Irthing-South Tyne watershed (Fig. 3). This is associated with a branching complex of glaciofluvial deposits, with one arm trending SW towards the Brampton kame belt and one arm trending NW towards Scotland (Trotter, 1929; Fig. 3). Feeding into the Brampton kame belt from the south is a network of SE-NW orientated meltwater channels cutting obliquely downslope in a northward direction

along the Pennine escarpment (Fig. 3, 4) (Trotter, 1929; Arthurton & Wadge, 1981; Clark *et al.* 2004; Evans *et al.* 2005; Greenwood *et al.*, 2007; Livingstone *et al.*, 2008). These have been previously interpreted either as a series of aligned marginal channels (Trotter, 1929) or as a predominantly subglacial drainage network with lateral and ice marginal feeder channels higher up on the escarpment flanks (Arthurton & Wadge, 1981; Greenwood *et al.*, 2007).

Methods

Geomorphological Mapping

Geomorphological mapping of the Brampton kame belt and surrounding area involved the recognition and compilation of discrete landform assemblages both on NEXTMap 5 m resolution airborne Interferometric Synthetic Aperture Radar (IFSAR) imagery (http://www.neodc.rl.ac.uk/), and digitised, geo-rectified aerial photographs (Cambridge University). The data was organised into National Grid tiles of 10 x 10 km based on Ordnance Survey co-ordinates. These data have been acquired by the British Geological Survey (BGS) for NERC and are archived at the NERC Earth Observation Data Centre (NEODC). Landforms were identified, based purely on morphological characteristics, into ridges (vectors), meltwater channels (vectors) depressions (polygons) and flat-topped hills (polygons). Mapping was carried out manually using on-screen digitisation. Layers were draped over the NEXTMap and aerial photograph imagery to: (a) display topographic contours (created from the NEXTMap DSME); (b) remove anomalous human artefacts (Ordnance Survey); (c) reveal the digitised results of the Glacial Map of Britain (Clark *et al.*, 2004; Evans *et al.*, 2005); and (d) illustrate both the superficial sedimentary deposits and bedrock geology (BGS) within the field area.

Sedimentology and Stratigraphy

Borehole information and exposures in both ridges and flat topped hills at Kirkhampton and Faugh sand quarries in the Brampton kame belt have been used to interpret depositional environments for the various geomorphological features. Texture, sedimentary structure, colour, bed geometry, contacts and inclusions were all measured and logged, from which lithofacies associations were identified. Scaled section sketches were drawn at the larger exposures so that the lateral extent of the lithofacies could be assessed. Paleaocurrent indicators (such as ripples and imbricate gravel), and clast lithologies augmented the sedimentary logging. Additional sedimentological and stratigraphic data from exposures in other sand quarries was obtained from Huddart (1970). Borehole logs (Jackson, 1979) provided a less detailed but wider coverage, allowing regional stratigraphic correlations.

Geomorphology

The geomorphology of the area is displayed in Fig. 5 and can be sub-divided into four principal assemblages, namely ridges, depressions, flat-topped hills and meltwater channels.

The first morphologically distinct feature comprises a complex system of ridges that occur throughout the entire kame belt. Most ridges wrap around the Pennine escarpment, trending SW-NE and then W-E around the northern-most section of the kame belt leading into the Tyne Gap (Fig. 5). A secondary SE-NW trend of a more subdued series of ridges is apparent, especially in the aerial photographs (Fig. 6a). The ridges are discontinuous, with lengths ranging from less than 100 m to over 2 km and heights of generally no more than 20 m and often more subdued (Fig. 6b). One exception is the larger, more prominent SW-NE aligned ridge at Brampton, to the north-west of the complex, which rises to 50 m, is 370 m wide and extends for 1.5 km. Ridges tend to be smaller, more discontinuous and with higher levels of complexity to the south-east of the kame belt. In places the ridges are anastomosing, as in the region of Carlatton Mill but most are branched, becoming increasingly dendritic northwards. Despite generally running along the contours of the slope, the ridges also display undulatory long profiles where they cross undulatory terrain, suggesting that streams responsible for their deposition were under hydrostatic pressure at least in places and at some time during the emplacement of the kame belt. The ridges themselves are situated at various heights in the kame belt, ranging from less than 100 m O.D. at the westernmost end to 200 m O.D. where the Hallbankgate esker (Fig. 3, 5) winds into the Tyne Gap.

Second, a series of circular depressions can be found throughout the kame belt but are especially prominent in the south-east where the terrain appears pockmarked (Fig. 5). They often punctuate ridges, thereby producing an undulating crest-line or discontinuous ridge form (Fig. 5, 6b). Depressions also occur on flat-topped hills. The depressions range from 20 m to 750 m in diameter, the largest being Talkin Tarn (Fig. 5), although most are between 20 - 60 m wide.

Flat-topped hills up to 1 km wide and 20 m high make up the third landform assemblage. The biggest of these occur at Stonebridge, Whin Hill, Cowran, Cote Hill, Netherton and just west of Talkin Tarn (Fig. 1, 5). Flat-topped hills are generally associated with ridge networks which are sometimes partially buried by the hills. Circular depressions are also common on the flat-topped hills. The flat-topped hills tend to occur within a central zone of the Brampton kame belt measuring 1.5 km wide by 6 km long, where they lie in close proximity to each other (Fig. 5) and range in height from 105 m O.D. to 140 m O.D.

Finally, meltwater channels occur but are generally rare within the kame sequence, although a few south-north orientated channels exist on the lower slopes of the Pennine escarpment. Another channel cuts SE-NW towards the bottom of the kame belt at Carlatton Mill (Fig. 5). On the south-eastern margin of the Brampton kame belt a series of SE-NW orientated channels cut into the kame topography giving it a ridged appearance (Fig. 5). This forms the northern edge of a major meltwater system running along the edge of the Pennine Escarpment and stretching as far south as the Stainmore Gap (Fig. 5, 7) (cf. Livingstone *et al.*, 2008). There are three major channel forms within the drainage network (Fig. 7) all of which cut into the Permian and Triassic bedrock. Type 1 channels are typically 'U' shaped, deeply incised and continuous, and can be traced for over 4 km in some instances. They also exhibit undulatory long profiles (Fig. 7). They form an anastomosing network of roughly parallel channels trending SE-NW (Livingstone *et al.*, 2008). Type 2 channels are generally smaller (< 1 km) and trend perpendicular to the hillslope gradient, orientated in a more northerly direction. These channels lack the undulations seen within the

Type 1 channels (Fig. 7). Finally, Type 3 channels are small (< 400 m) and deeply incised and plunge westwards, from inception points generally associated with the Type 2 channels (Fig. 7). The south-western edge of kame belt is linked to a few short (*ca*. 400 m) SW-NE orientated channels which cut across the Penrith sandstone escarpment. The north-eastern arm of the Brampton kame belt feeds into (via the Hallbankgate esker) an 8 km long, deeply incised meltwater channel that cuts across the watershed into the Tyne Valley system. The channel possesses undulations in the western end as it crosses the watershed, before gently dipping down into the South Tyne Valley.

Sedimentology and stratigraphy

Ridges

Several exposures have been logged through ridges within the Brampton kame belt. These include a quarry at Kirkhampton near Milton, two sites used by Huddart (1970) at Brampton ridge and Quarrybeck and a site north of Whin Hill. These exposures are augmented with borehole data collected by the British Geological Survey (Jackson, 1979).

Site 1: Kirkhampton

Kirkhampton sand and gravel quarry (NY 563 601) is located east of Milton in the northern kame belt region (Fig. 1). The western end of the quarry leads into a W-E orientated ridge, 300 m long and 140 m O. D. The quarry contains 4 major lithofacies associations (LFA) which are outlined diagrammatically in Figure 8 and are described and interpreted in turn below.

Lithofacies Association 1 (LFA K1; series of gravel channel fills and trough cross-bedded sand and gravel) - description:

Lithofacies association 1 (LFA K1) is characterised by 0.2 - 1.5 m thick tabular cross-beds and planar beds of fine-coarse sand, a series of vertically stacked trough cross-beds ranging from 0.5 - 5 m in width and clast-supported gravel channels up to 0.5 m thick and 5 - 10 m wide (Fig. 8, 9a, b). The trough cross-beds exhibit fining upwards sequences from stratified coarse sand and granule gravel (with some pebble gravel) into fine-medium sands. These structures often cut-across the tabular cross-beds and planar beds of fine-coarse sand (Fig. 9a, b) which contain outsized clasts. The gravel channels, which are generally found towards the bottom of the LFA, have an erosional base and are predominantly structureless apart from infrequently observed centimeter-scale lenticles of sand. LFA K1 is rarely found throughout the quarry, with sequences generally vertically stacked (up to 10 m thick) between and within LFA K2 and K3. Bounding surfaces are characterised by marked shifts in grain size, bedform scale and lithofacies type, with frequent erosional surfaces.

LFA 1 - interpretation

The stacked multi-storey sequences of LFA K1 indicate that vertical accretion was the prevalent depositional mechanism (Collinson, 1996). The sets of trough cross-beds result from the filling of channels by migratory sand dunes in a low energy environment (Miall, 1977), while planar-bedded sand demonstrates transport as a traction carpet in the upper-flow regime (Miall, 1977; Allen, 1984). Gravel at the base of the troughs is associated with erosional re-activation of the facies, with upwards fining eventually leading to abandonment (Smith, 1985). Pebble-gravel channels indicate bedload transport, possibly as channel lags or channel bars, from high energy stream flows (Collinson, 1996). The lithofacies association is therefore indicative of a fluvial environment characterised by aggradation and then abandonment of channels and reflecting channel, dune and bar migration in a fluctuating hydrological regime typical of braided rivers (e.g. Williams & Rust, 1969; Rust, 1972; Miall, 1977).

Lithofacies association 2 (LFA K2; laminated sands and ripple structures) - description

LFA K2 (S2A & B, Fig. 8) comprises a series of fine sand laminations characterised by fining-upwards sequences, ripple structures and out-sized granule-pebble gravel (Fig. 9c). This lithofacies association is infrequently observed and generally interbedded within LFA K1 and K3. Thicknesses rarely exceed 2 m whilst bed widths are generally greater than 10 m. Ripples are typically found at the base (and infrequently at the top) of the lithofacies and include: gently sloping (< 10°), laterally discontinuous type 'A' climbing ripples (Jopling & Walker, 1968); and fine-grained sinusoidal ripples up to 5 cm thick (Fig. 9C). Palaeo-current directions are variable, although the general trend is towards the NNE (S2B, Fig. 9c).

LFA 2 - interpretation

The horizontally laminated sand is interpreted to have formed by low energy traction currents during planar bed flow (Jopling & Walker, 1968; Smith & Ashley, 1985). The development of type 'A' climbing ripples, at the top and base of the lithofacies association, demonstrates the waxing and waning flow of water respectively (Miall, 1985), with an increase in suspended sediment input and a reduction in flow velocity relative to the horizontal laminations. Fine-grained sinusoidal ripples demonstrate deposition predominantly by suspended sediment rain-out in very quiet waters (Jopling & Walker, 1968; Allen, 1973; Ashley *et al*., 1982). The palaeocurrent data suggests that flow generally trended NNE, although with significant variability. Thus the LFA is indicative of a low energy environment characterised by variations in the suspended sediment input and flow velocity.

Lithofacies Association 3 (LFA K3; series of tabular cross-bedded stratified sand and fine gravel, draped clay/silt bands and pebble gravel) - description

LFA K3 (S1, 2B, 3 & 4, Fig. 8) is composed of tabular cross-beds of stratified medium-coarse sand and granule gravel with drapes of clay/silt and occasional pebble gravel lithofacies (Fig. 9d). Stratified medium-coarse sand and granule gravel facies are *ca.* 0.8 m thick and dip at various orientations from the north to the northeast at angles ranging from 18-30°. Each dipping unit is

bounded by an erosional re-activation surface. Massive, coarse sand containing granule-pebble gravel up to 0.5 m thick is often observed (Fig. 9d), whilst there are also rare, shallow (< 1 m) granule-pebble gravel lithofacies that display trough and lenticular geometries and erosional lower surfaces. Occasional fine-grained drapes up to 15 cm thick and with undulatory profiles are observed at irregular intervals throughout the lithofacies association (Fig. 9d), with the greatest frequencies (and thicknesses) at the eastern end of the quarry. LFA K3 is the dominant sedimentary association within the quarry reaching thicknesses of up to 15 m and extending throughout the quarry.

LFA 3 - interpretation

The tabular cross-bedded stratified sand and granule gravel lithofacies are interpreted as dune forms (Miall, 1977) analogous to the deeper portions of active channels where the bedload is predominantly sand; the lateral extent and range in orientations indicative of a broad, unconfined channel (Miall, 1985). Vertical accretion of discrete co-sets bounded by re-activation surfaces is typical of migratory dune formation (Banerjee & McDonald, 1975). The interbedded coarse sand with granule-pebble gravel could be interpreted as antidunes (Shaw, 1972), thus suggesting that deposition occurred sub-aerially (Banerjee & McDonald, 1975). The irregularly spaced clay bands were formed by the settling out of fines, which therefore demonstrates evidence for the periodic, pervasive shut-down of the fluvial system (Miall, 1977). These dune bedforms, which show evidence for continual re-activation, migration and vertical accretion, could form in a low flow, braided river system characterised by fluctuating discharge (Miall, 1977).

Evidence for deformation - description

Deformation is persistent throughout LFA K1, 2 and 3, with the most extensive evidence at the base of the vertical sequence (S1, 2 & 4, Fig. 8). This includes 5 - 10 m wide by 2 - 5 m deep open folds (S1, 2 & 4, Fig. 8) characterised by high angle reverse faults (with offsets of up to 5 cm), overlapping facies, over-steepened stratified sand and granule gravel, truncated facies, and a series of normal faults (millimeter - centimeter scale) along the crest of the folds (S2, Fig. 8), often arranged *en echelon*. Indeed normal faulting is common throughout the quarry, often characterised by block failure (Fig. 9e), while there is also extensive evidence of centimeter-scale incorporation, soft sediment pods, stringers, ball and pillow, water escape and flame structures (S1, Fig. 8), and displaced blocks of sand within the stratified sand and granule gravel.

Evidence for deformation - interpretation

Vertical deformation structures such as the open folds and block failures are associated with collapse of the depositional floor owing to the melt-out of buried ice blocks (McDonald & Shilts, 1985; Krüger, 1994; McCarroll & Rijsdijk, 2003) at a variety of scales. The preponderance of normal faults and displaced blocks of sediment is indicative of gravitational failure with the displaced blocks analogous to bank collapse. High pore waters must have existed either during or following deposition due to the presence of stringers, water escape, ball and pillow and flame structures.

Kirkhampton Ridge synopsis: environment of deposition

The sedimentary lithofacies associations at Kirkhampton sand and gravel quarry (Fig. 8, 9) are envisaged to have been deposited in a broad, unconfined, glaciofluvial braided channel resting on dead ice (cf. Price, 1966; Bennett & Glasser, 1996; Huddart *et al.*, 1999). The braidplain consisted of co-sets of dunes (sand flats) associated with unsteady, unconstrained flow undergoing periodic re-organisation and occasional abandonment (LFA K3), and regions of more persistent flow (LFA K1) where migratory channels dominated (cf. Nemec, 1992). The complex shifts in grain size, facies and lithofacies associations and the reactivation surfaces are indicative of glaciofluvial outwash undergoing fluctuating discharge, channel migration and pulsed incision (e.g. Owen, 1997). The prevalence of dead-ice structures and outsized clasts (which in this context were probably deposited as drop-stones) throughout all the lithofacies associations suggests that the glaciofluvial outwash was in contact with ice (Shaw, 1972; Huddart *et al.*, 1999). Bank failure blocks and gravitational slumping indicate that the environment was very unstable, whilst the presence of ball and pillow and flame structures demonstrate mass-flowage and collapse of the upper facies due to dead ice disintegration, leading to the loading and de-watering of fine grained material (cf. Cheel & Rust, 1982; Donnelly & Harris, 1989; Mager & Fitzsimons, 2007).

Site 2: Brampton Ridge (BR), Quarrybeck Pit (Huddart, 1970)

Description

Brampton ridge forms the most prominent feature of the kame belt, running north-east from Brampton for 0.9 km and rising 50 m, with peaks of 120 m O. D. on its undulating crest (Fig. 1, 5). The ridge is located in the northerly-most region of the kame belt with the quarry situated in the very north-eastern edge of the ridge (NY 543 623). Huddart (1970) collected 3 logs in the exposed face, which are reproduced here in Figure 10.

The stratigraphy is composed predominantly of sand, but with a general upwards coarsening into a pebble-gravel facies at the top. Below the currently exposed sequence Huddart (1970) observed red clay which he interpreted as basal till (Fig. 10). Three major lithofacies associations were observed within the sequence. LFA BR1 comprises rippled fine sand with a maximum thickness of 35 cm, interbedded with horizontally stratified medium-coarse sand dipping at 5° to the north-east, thin clay bands and silt layers. LFA BR2 comprises 2.66 m of horizontally stratified, coarse sand with thin pebble layers and erosional scours. Cross-stratification is also evident in the lower part of LFA BR2, with foreset dips of 10° and a palaeo-current indicating deposition from the south-west (Huddart, 1970). The final lithofacies (LFA BR3) is composed of 55 cm of pebble-gravel dipping at 5°.

Interpretation

Deposition of horizontally stratified sand and ripple structures at the base of the sequence is indicative of a low energy flow regime (Collinson, 1996). The horizontally stratified sand is envisaged to have formed by planar-bed flow in shallow water (hence preventing dune development), possibly as a result of sheet flooding (Miall, 1985; Collinson, 1996). The progressive coarsening up-sequence into pebble gravel is indicative of bar and channel development in the upper flow regime, and palaeocurrents suggest that flow was parallel with the north-east orientation of the ridge. The exposure at Brampton ridge is therefore interpreted to have been deposited in a fluvial channel, which, because it is located in an upstanding ridge, must have been ice-walled (cf. Price, 1969, 1971, 1973).

Site 3: Braithwaite's sand and gravel pit (Huddart, 1970)

Description

Braithwaite's sand and gravel pit (NY 512 568) is situated in a 300 m SW-NE trending ridge north of Whin Hill (Fig. 1, 5). Huddart managed to log both the lateral and vertical extent of the ridge (Fig. 11). The central axis of the ridge (logs 5 and 6) grades up through a red, sandy clay lithofacies containing diamicton balls into 4 m of large scale, trough cross-stratified coarse sands, 5 m of large pebble-gravel filled channels, 2.3 m of imbricate pebble-gravel and 3 m of horizontally stratified coarse sands. Exposures on either side of the ridge axis are dominated by alternations of horizontally stratified coarse sand, tabular cross-stratified sand, fine grained bands and sinuosidal and type 'A' ripple-drift cross-laminated sand (Jopling & Walker, 1968). The tabular cross-stratified lithofacies have foreset dips ranging from 22 - 26°. Marginal faults dipping towards the south-southeast are evident below the top unit of pebble-gravel, between logs 5 and 7 in the marginal zone of the ridge. Palaeocurrents are varied, ranging from east to north-east in the faulted gravel, to west in the tabular cross-stratified sand.

Interpretation:

The exposures through the central axis of the SW-NE trending ridge are indicative of a high energy flow regime, where trough cross-stratified coarse sands represent dune forms (Miall, 1977). The horizontal sand is interpreted as an upper flow regime shallow sheet flood deposit. The gravel lithofacies represent either channel scour or bar deposits, with imbricate gravels indicating traction deposition (Miall, 1977, Collinson, 1996). Thus the central exposures record fluvial deposition typical of a braided stream (e.g. Miall, 1977) characterised by fluctuating, unsteady and high energy flow (Collinson, 1996). The deposits towards the ridge margin indicate deposition in the lower flow regime, with shallow angled tabular cross-stratified sand thought to represent dune formation in the lower flow regime (Miall, 1977). The horizontal coarse sand is interpreted as a sheet flood deposit (Collinson, 1996) and alternations of sinuosidal ripples and fine-grained drapes are analogous to suspended sediment rain out. Type 'A' climbing ripples record a relative reduction in suspended sediment and an increase in bedload transport (Jopling & Walker, 1968; Allen, 1973; Ashley *et al.*, 1982).

Boreholes: Mineral Assessment Report 45

Borehole data (Jackson, 1979) through ridges at Hall Bank (NY 551 588) and Tarn End (NY 543 580) (Fig. 1) provide additional stratigraphic and sedimentological information from the depositional ridges (Fig. 12). A red-grey till containing shale and sandstone is evident in the bottom 2.1 m of Hall Bank borehole. Sands and gravels within the ridges are up to 13.2 m thick. At Hall Bank the basal 1.2 m comprise gravel and occasional boulders, followed by 1.4 m of massive red sandy silt and then 6 m of sand (Fig. 12). This documents an abrupt change in discharge regime during the early stages of ridge deposition. Deposits at Tarn End comprising more than 6.5 m of pebbly sand followed stratigraphically by 6.7 m of gravel (with clay at the very top) are indicative of a high energy fluvial system.

Synopsis of quarry exposures, and borehole data in ridges: environment of deposition

Stratigraphic and sedimentological evidence collected through ridges in the Brampton kame belt can be reconciled with a fluvial regime characterised by unsteady, migratory flow (cf. Miall, 1977, 1985; Owen, 1997). Marginal faults and the presence of 'till' balls at Braithwaite's sand and gravel pit suggests that the ridge was in contact with an ice mass (Huddart, 1970; Shaw, 1972; Gustavson & Boothroyd, 1987; Warren & Ashley, 1994). Marginal faults are envisaged to have been formed by gravitational collapse due to the removal of a supporting ice wall (McDonald & Shilts, 1985). A typical trend seems to be that of a central channel forming along the axis of the ridge characterised by vertical accretion of dune forms and incised channels in a high energy, unsteady flow regime, together with shallow sheet flow, characterised by periodic channel abandonment, and water depth fluctuations along the ridge margins. The presence of both normal and reverse grading is a product of a highly variable discharges, whereby continual abandonment and reactivation results in some channels becoming major conduits (coarsening upwards), whilst others devolve into small backwater outlets (fining upwards). Similar lithofacies associations in sinuous ridges have been previously reported from eskers (e.g. Shaw, 1972; Warren & Ashley, 1994), wherein esker cores often display cyclic sequences of gravel and sand (Bannerjee & McDonald 1975; Ringrose 1982; Brennand 1994; Brennand & Shaw 1996). Fining-upward sequences with erosive bases record fluctuations in discharge and sediment availability, and the depositional cycles (rhythmicity) have been interpreted as both annual (Bannerjee & McDonald 1975; Mäkinen 2003) and seasonal (Brennand 1994).

Horizontal facies variability is also common in situations where eskers contain cavity fill sequences, produced when tunnels widened, either due to flotation in proglacial lakes (e.g. Gorrell & Shaw 1991; Brennand 1994, 2000) or leakage of tunnel waters into lateral, ephemerally water-filled cavities (e.g. Gordon et al. 1998; Mair et al. 2002). The latter have been linked to the construction of anabranched reaches, subaqueous fans and hummocky zones along otherwise predominantly single ridged eskers by Brennand (1994, 2000). Fining outwards from the main ridge is thought to represent side-wall melting and esker widening, an interpretation supported by the occurrence of faulting. An esker may be "widened" by sediment draping where discharge from the tunnel portal is into a subaqueous environment, which may be at the flotation point in a proglacial lake or where the tunnel exits into a supraglacial pond.

Flat-topped hills:

Several exposures have been logged through flat-topped hills (Fig. 1, 5) within the Brampton kame belt. This includes a sand pit at Faugh, a site at Whin Hill (Huddart, 1970) and borehole data collected by the British Geological Survey (Jackson, 1979).

Site 1: Faugh sand pit:

Faugh sand pit (NY 514 550) is located at Whin Hill (120 m O.D.), to the northeast of Faugh village. Whin Hill is a 710 m long and 590 m wide flat-topped hill standing up to 20 m above the surrounding landscape. Ridges, orientated northwards, run into and out of the hill (Fig. 5). Four major lithofacies associations have been identified in the stratigraphic section and these are outlined diagrammatically in Figure 13.

Lithofacies Association 1 (LFA F1; series of fine sands, silts and clays) - description

At the base of the sequence in the north-western corner of the sand pit (S1, Fig. 13), and also higher up in the northern section of the pit (S4, Fig. 13), facies are dominated by alternations of horizontally bedded clay, silt and fine sand, massive fine-medium sand (Fig. 14e) and type 'B' climbing ripples, which often grade up into sinusoidal climbing ripples (Jopling & Walker, 1968). The climbing ripples dip at an angle of 18°, with a general orientation of 322° (palaeocurrent towards the north-west). Individual facies vary in thickness from as little as 5 cm to over 1 m, whilst the overall thickness of the sequence is *ca*. 6 m thick. Evidence of deformation includes centimeter scale folding, faulting and incorporated boundaries.

Further to the south (S2, Fig. 13), exposures reveal 4 m of WNW dipping (30°) sand, parallel laminated clay and sand, massive sand containing granule-gravel, and silt and clay bands up to 30 cm thick (Fig. 14c). In the bottom 50 cm of the exposure a series of clay, silt and sand laminations are truncated by stratified sand. The dipping sands are bounded by horizontal clay bands. There is evidence for deformation throughout the S2 exposure, with incorporated, convoluted silt and sand in the lower 50 cm, and a series of centimetre-scale fault structures and warped silt layers in the upper sequence. Just to the south-east of the exposure a meter-scale normal fault is also evident.

LFA 1 - interpretation

Sediments in LFA F1 are interpreted to have been deposited in a low energy environment. The sinusoidal ripples, clay-silt laminae, clay bands and laminated fine sands are indicative of rapid suspension settling within quiet waters (Jopling & Walker, 1968; Ashley *et al*., 1982). Upward transitions from sinusoidal to type 'B' ripples are consistent with an increase in bedload transport relative to suspension fall-out (Jopling & Walker, 1968), whilst horizontally bedded and coarser sand indicate a change to low density turbidity currents (Reineck & Singh, 1975; Allen, 1984; Smith & Ashley, 1985). Palaeocurrent data indicate that flow was towards the northwest.

Evidence of cross-bedded sand with minor granule gravel at S2 (Fig. 13) is typical of foreset aggradation, abandonment and reactivation (Smith & Ashley, 1985). The alternations between facies type exhibited within LFA F1 suggests that the depositional environment was constantly in flux, with a variety of processes, including density underflows, suspension settling, turbidite sedimentation and foreset progradation taking place.

Lithofacies Association 2 (LFA F2; cross-bedded sands with upper fine-grained drapes) - description

Stratigraphically positioned above LFA F1 are a series of shallow-angled, cross-bedded sands that display a variety of orientations, and are bounded by erosional lower contacts. Occasional shallow, metre-scale cut and fill structures composed of sand are also evident throughout the sequence. These facies are overlain by drapes of fine-grained sand and clay bands which exhibit a cyclical series of climbing ripples and planar sand laminations (S4, Fig. 13).

LFA 2 - interpretation

LFA F2 is interpreted as the deposit of a low energy, highly variable fluvial system. The cross-bedded sand is characteristic of dune forms (Miall, 1977), with the various orientations of the dunes indicative of transient, unconfined inflows into the system. Vertical accretion of discrete co-sets bounded by re-activation surfaces demonstrates dune migration (Banerjee & McDonald, 1975). The shallow angled cut and fill sequences are symptomatic of higher energy scouring from underflows (Collinson, 1996), whilst the return to fine-grained drapes of laminated fine sand and climbing ripples as seen in LFA F1, suggests that the final stages of deposition were dominated by suspension in standing water and low energy traction currents (Jopling & Walker, 1968; Smith & Ashley, 1985).

Lithofacies Association 3 (LFA F3; sands and gravels with incorporated diamicton) - description

Situated in the north-eastern corner of the flat-topped hill, LFA F3 is dominated by laminated, cross-bedded and massive sand, gravel channels and interbedded diamicton (S3, Fig. 14a). The bottom 1 m of the section is composed of laminated sand and coarse, massive sand. In the eastern-most exposures the sand grades up through massive red silt, into a 1 m thick, 'spoon-shaped' channel composed of pebble-cobble gravel and coarse sand, which pinches out at either end (S3D, Fig. 13), and fines upwards and outwards away from the scour bottom. Gravel within the channel reaches diameters of up to 20 cm, and is composed almost exclusively of Permo-Triassic sandstone. The bottom contact with the silts is erosional, with evidence for both incorporation and normal faulting. The gravel channel grades up into a *ca*. 2 m thick stratified sand and gravel sequence, dipping towards the west, horizontally aligned granule gravel facies and massive coarse sand (S3C, Fig. 13).

West of the gravel lithofacies and stratigraphically positioned above the massive sand lithofacies is a diamicton. The diamicton is 1.3 m thick, massive, with a red-brown (2.5YR 3/3), sandy-silty,

matrix-dominated texture and a soft to firm composition (Fig. 14b). Clasts are rounded to sub-rounded and up to 10 cm in diameter, although generally scarce. Larger clasts are generally positioned towards the middle of the lithofacies, with the upper 40 cm containing 1 - 3 cm (diameter) soft sediment inclusions. The diamicton unit dips down towards the west (towards LFA F1 & 2), pinching out at both ends with an interbedded (sheared) lower contact (Fig. 14b). Resting on the diamicton are sand and laminated silt facies (showing evidence of truncation), and a very coarse sand and granule gravel fining upwards into cross-bedded sequences typical of LFA F2 (S3A, Fig. 13). The finer sands contain a series of 20 - 30 cm contorted clay-silt structures, characterised by recumbent folds. Balls of diamicton have been incorporated within the sand facies lying directly on top of the interbedded diamicton.

LFA 3 - interpretation

The series of laminated and massive, coarse sand lithofacies are analogous to deposition by low density turbidity currents (Reineck & Singh, 1975; Allen, 1984; Smith & Ashley, 1985) with the massive sands probably associated with sediment gravity flows (Eyles, *et al.*, 1987). The incorporated contacts and westerly dipping lithofacies support this interpretation (Lawson, 1979, 1981, 1982). The thickness (1.3 m) and geometry of the diamicton coupled with the small shear zone of incorporated and deformed material at the base is indicative of a debris flow (Lawson, 1979, 1982). Soft sediment pods are thought to have formed by the incorporation of ponded subaerial material (Lawson, 1982). The series of massive sand, laminated fine sand and normally graded coarse-fine sand resting on-top of the diamicton are again interpreted as sediment gravity flows associated with turbidity currents, with the recumbent fold structures, convolute bedding and diamicton balls supporting this notion (Lawson, 1981, 1982). The gravel channel, exposed to the east of the diamicton, has a geometry typical of a scour structure, with interdigited sand and granule-pebble gravel in the shallow part of the scour and fining upwards typical of a channel bend, characterised by lower energies and point bar growth down the avalanche face in the inner bend, and high energy scour conditions in the thalweg (Miall, 1985). Westwards dipping, tabular cross-beds of coarse sand and granule gravel were probably formed by dune accretion (Miall, 1977, 1985; Collinson, 1996).

Lithofacies Association 4 (LFA F4; gravel channels and cross bedded gravel and sand) - description

The eastern corner of the quarry, is characterised by interbedded NNE dipping (32°) stratified coarse sand with granule gravel, clast-supported granule gravel and clast-supported pebble gravel (with each lithofacies less than 0.4 m thick), occurrences of clay balls and gradational contacts (S5A, Fig. 13). This leads stratigraphically into *ca.* 1 m of massive coarse sand with some granule gravel, followed by a 0.55 m thick pebble-cobble gravel channel fill characterised by an erosional basal contact and gradational fining into dark-red fine sand and silt (S5B, Fig. 13). The gravel channel is over 10 m wide, pinching out at either end, with a flat basal contact (Fig. 14d), and represents one of many similarly formed gravel facies. Imbrication within the gravel facies is orientated towards the northwest (330°), with cobbles up to 20 cm diameter. The gravel lithofacies contains evidence of normal faulting, with offsets of up to a meter, diamicton balls,

and rare blocks of sand *ca*. 30 cm thick. Lying stratigraphically above this sequence, in the very north-east of the quarry, are further massive, pebble-cobble gravel channels containing inter-fingered sand lithofacies and heavily faulted laminated fine sand with occasional outsized granule-gravel clasts (Fig. 14f). The faults are normal and downthrow is towards the WSW and ENE at dips of 50-70°. They extend up into the gravel channels and have offsets ranging from centimeter to meter scale (Fig. 14f). The massive gravel deposits have erosional lower contacts.

LFA 4 - interpretation

The dipping, stratified, coarse sand and granule-pebble gravel is thought to represent lateral accretion of a transverse bar form, 1.5 m thick (Collinson & Thompson, 1989). The beds dip obliquely from the general palaeocurrent direction displayed in the imbricated upper gravel facies, indicating lateral shoreward accretion, which is typical of transverse bars (Boothroyd & Ashley, 1975; Miall, 1977, 1985; Collinson & Thompson, 1989). The cyclical nature pertaining to pulsed changes in flow velocity and depth is elucidated from the facies organisation (Miall, 1985; Collinson & Thompson, 1989). The massive nature of each individual facies could result from rapidly fluctuating discharges during which the sediment concentrations were high (Collinson & Thompson, 1989). Flat, long channel geometries with tapered ends, imbrication and massive gravel beds is demonstrative of longitudinal bar deposition dominated by bed-load transport in a fluid flow (Miall, 1977, 1985). Gravel imbrication demonstrates traction deposition towards the NW with flow thus corresponding to the orientation of the ridge north of the exposure. Fining upwards sequences suggest gradual abandonment of bars (Miall, 1977), whilst blocks of sediment within the bars probably resulted from bank failure. Coarse grained sand and granule gravel, within which these bars are deposited, is symptomatic of a high energy, non-cohesive and sediment rich fluvial system. The uppermost facies, composed of interdigited horizontally laminated sand and massive gravel, demonstrates deposition in the upper flow regime. The horizontal sand laminations were deposited during planar flow conditions (Allen, 1984, Collinson, 1996), and the sheet gravels resulted from high competence, rapidly accreting, rising stage flows, possibly as a result of a major flood event (e.g. Russell *et al*., 2001). As the gravels are interfingered with the sand facies it suggests that these gravel channels originated within a central zone, and then accreted laterally across the braidplain during rising stage flow. The normal faults indicate vertical collapse of the depositional floor (McCarroll & Rijsdijk, 2003), possibly due to the melt-out of underlying dead ice. The orientation of the faults (striking transverse to the general palaeocurrent direction and ridge orientation) is typical of marginal collapse caused by the removal of ice-supporting walls (McDonald & Shilts, 1975).

Site 2: Whin Hill, Faugh sand and gravel pit (Huddart, 1970)

Huddart (1970) investigated Faugh sand pit at Whin Hill (NY 515 552), although only the top 6.2 m were exposed when he gained access (table 1).

Dip	*Stratigraphy*	*Thickness (m)*	*Depth (m)*

16°	Horizontally stratified, coarse sand with occasional pebble-gravel	1.7	1.7
16-18°	Horizontally stratified, coarse sand with occasional pebble-gravel	3.0	4.7
2°	Parallel lamination in silts and fine sands with slightly sinusoidal lamination and occasional pebble-gravel	1.5	6.2

Table 1: Whin Hill, Faugh (Huddart, 1970)

The exposure displays structures which are typical of a deltaic sequence including fine grained, parallel laminated sand (1.5 m) analogous to bottomsets, and dipping, stratified coarse sand with pebble gravel (3.0 m), which are characteristic of foreset structures (Smith & Ashley, 1985). Imbricate gravel at the site gave orientations of 205° (Huddart, 1970) suggesting that the sequence prograded in a north-easterly direction, similar to that of the linear ridges. Fault structures identified throughout the sequence indicate vertical collapse of the depositional floor (McCarroll & Rijsdijk, 2003).

Borehole Data:

Borehole data (Jackson, 1979) was obtained from Crews (NY 533 586), Netherton (NY 541 569) and Whin Hill (NY 514 553) (Fig. 1 & 12). The boreholes reveal a series of silt, fine-coarse sand and sandy gravel facies, with vertical aggradations up to 25 m thick and a general coarsening upwards (Fig. 12). At Whin Hill a thin (1.3 m) bed of diamicton is interdigited between the sands and gravels. Thus deposition is thought to have occurred in a low energy environment (Collinson, 1996), with the presence of diamicton demonstrating the proximity of ice.

Synopsis of quarry exposures and borehole data of flat-topped hills: depositional environment

The stratigraphic architecture and characteristics of the lithofacies associations exposed at Faugh sand pit are analogous to the infilling of a former ice-walled lake plain (cf. Smed, 1962; Clayton & Cherry, 1967; Ham & Attig, 1997; Johnson & Clayton, 2003, Clayton *et al*., 2008). The central zone of the mound (LFA F1 & 2) is characterised by rhythmically bedded fine-grained sediments, drop-stones and a general absence of deformation, typical of bottomsets (Smith & Ashley, 1985; Clayton *et al*., 2008). These grade up into sand-dominated cut and fill sequences and dune bedforms, representing low energy glaciofluvial flow across the lake floor from a variety of directions during the final stages of infilling. The marginal deposits are generally coarser, with evidence of debris flows composed of diamicton and sand dipping towards the centre of the lake, as typified by other relict lake plains (e.g. Clayton & Cherry, 1967; Clayton *et al*., 2008). Foreset structures at Whin Hill could represent a small deltaic sequence (Smith & Ashley, 1985; Aitken, 1995) which probably extended into either an ice-walled lake plain (e.g. Clayton *et al*., 2008) or

supraglacial lake (e.g. Mager & Fitzsimons). The coarsening upwards, fine-grained sediments exhibited within the boreholes have a similar sedimentology to the sequences exposed at Whin Hill and Faugh, which suggests a similar origin, although the lack of detailed data on deformation and sedimentological structures does not allow confirmation of an ice-walled origin.

The gravel channels exposed in the north-eastern corner of Faugh sand pit (LFA F4) are envisaged to have been deposited in a broad, supraglacial or ice-walled, braided glaciofluvial trough characterised by migratory bar and dune development, lateral accretion and flood channeling (e.g. Gustavson & Boothroyd, 1987; Huddart, *et al.*, 1999; Russell *et al.*, 2001). The presence of till balls and vertical collapse structures supports this interpretation (Shaw, 1972). Palaeocurrent data indicates that the glaciofluvial channel flowed in a north-easterly direction.

Discussion

<u>Geomorphology and sedimentology</u>

Geomorphological, stratigraphic and sedimentological analysis of the Brampton kame belt has enabled a number of key inferences to be made about the landform. We now provide a synopsis of our interpretations of depressions, ridges, flat-topped hills and meltwater channels based upon the geomorphic and sedimentological details of the field sites described and analysed above, and informed by modern analogues (see Fig. 15). This synopsis is then used to provide a depositional model for the Brampton kame belt.

Depressions are interpreted as kettle holes, formed by the melt-out of areas of dead ice underlying glacigenic sediment (e.g. Clayton, 1964; Price, 1971, 1973; Krüger, 1994; Evans & Twigg, 2002). The prevalence of kettle holes and the sedimentological evidence for widespread faulting and subsidence throughout the region is construed as verification of extensive ice cored sedimentary deposition, followed by topographic inversion during ablation. This sort of environmental setting comprising ice-cored glacigenic outwash is commonly observed along the margins of modern glacier snouts fed by significant volumes of meltwater such as those in Iceland (Fig. 15). Sedimentological and stratigraphic evidence of folding and faulting at both Kirkhampton and Faugh sand pit, combined with observations made by Huddart (1970), demonstrate the presence of vertical collapse structures throughout the lithofacies associations. This supports the notion of either melt-out of underlying dead ice or the removal of ice-supporting walls (Boulton, 1972; McDonald & Shilts, 1975; Johnson & Clayton, 2003). The geomorphology, which displays a series of kettle-hole features within ridges and flat-topped hills, supports this inference.

Ridges contain two discrete sedimentary successions, those at the ridge core and those in the ridge flanks. Ridge cores are generally composed of bars, dunes, channels and scour fills. These structures are typical of braided river deposits exhibiting unconfined flow, variable discharge and channel migration (Boothroyd & Ashley, 1975; Miall, 1977, 1985). Exposures in the ridge margins reveal a lateral fining into a series of dunes, planar bedded sand, ripple structures and fine-grained bands which are analogous to flow in a low energy glaciofluvial environment

characterised by fluctuating water depths and periodic abandonment. Extensive faulting both marginally (Brampton ridge, Whin Hill) and pervasively (Faugh) throughout the exposures suggests that ice-contact conditions prevailed (e.g. Price, 1969, 1971, 1973; Shaw, 1972; McDonald & Shilts, 1975). Thus these deposits are analogous to eskers formed in either a broad, supraglacial (e.g. Huddart & Bennett, 1997; Huddart *et al.* 1999; Russell *et al.*, 2001) or/and ice-contact (e.g. Huddart, 1970; Shaw, 1972) trough. Geomorphic evidence for complex dead ice disintegration is manifest in the beaded, discontinuous morphology and pockmarked terrain (cf. Price, 1969, 1971, 1973; Huddart & Bennett, 1997; Thomas *et al.*, 1998; Evans & Twigg, 2002). Despite individual ridge lengths rarely exceeding 1 km, networks of ridges can be traced along the entire length of the Brampton kame belt, thereby demarcating a series of beaded esker-like morphologies (e.g. Banerjee & McDonald, 1975). This undulating ridge morphology is archetypal of ice cored sediment undergoing differential melting, collapse and topographic inversion (Price, 1966, 1969, 1973; Boulton, 1972; Evans, 2009) and can be observed in evolving ice-marginal landsystems along the margins of Sandsfellsjökull, Bruarjökull and Fjalljökull in Iceland (Fig. 15b, c, e & f). These active margins demonstrate the temporal changes that ice-cored glacigenic sediments undergo as topographic inversion occurs, leading to the gradual disintegration of the ridge structure, localised ponding and debris flow reworking (Fig. 15). Marginally deposited debris flows composed of diamicton intercalated between glaciofluvial deposits, supports the interpretation of an ice-walled depositional environment.

The two major ridge orientations, together with associated palaeocurrents suggest that flow generally drained north-eastwards and north-westwards. This indicates that the meltwater drainage network was sourced in the Eden Valley and northern Pennines. There is some evidence for cross-cutting between the two orientated ridge systems, especially visible in the aerial photographs (Fig. 6a), which, when combined with the buried landforms, suggests that the kame belt formed either time transgressively in a series of stages as ice receded out of the Solway Lowlands or at various levels within the ice (i.e. supraglacially, englacially and subglacially). The Eden Valley/north Pennines provenance for the ridge material is verified by the clast lithological analysis (n = 300). The diamicton lithofacies at Faugh sand pit is composed of 47% Silurian and Carboniferous sandstone (sourced from the Southern Uplands and Vale of Eden), and then 7% Permo-Triassic sandstone, 4% Carboniferous Limestone, 6.5% Quartzitic sandstone, 6% mudstone and siltstone, 14% Borrowdale Volcanic Group lavas and 0.5% Threlkeld granite sourced from the Vale of Eden and Lake District. The gravel has a similar lithology, although with much less Silurian and Carboniferous sandstone (25%), and more Permo-Triassic sandstone (12%), Carboniferous Limestone (8%) and Borrowdale Volcanic lavas (30%).

Ridge networks are intimately associated with the other major geomorphological features (flat-topped hills and kettle holes) within the kame belt. Some ridges, trending in and out of the flat-topped hills, are partially buried, suggesting that flat-topped hills formed at a slightly later stage of deglaciation, but are related to the same glaciofluvial drainage system.

The Brampton kame belt exhibits a general fining westwards and northwards (Jackson, 1979). This trend can be reconciled with a southerly water source, coming off the Pennine escarpment and Penrith sandstone ridge depositing coarser material proximal to the active ice margin. This interpretation ties in with both the palaeo-current and provenance data. The southern zone of the

kame belt is dominated by chaotic hummocky sand and gravel deposits with little structure, thus suggesting that the dominant process was dead ice disintegration and topographic inversion consistent with a relatively thick ice core.

Flat-topped hills are interpreted as ice-walled lake plains, occasionally associated with ice-contact (supraglacial) deltaic sequences (cf. Smed, 1962; Clayton & Cherry, 1967; Johnson & Clayton, 2003; Clayton *et al.*, 2008). The central zone of the flat-topped hill at Faugh is composed of cyclical series of laminated sand, climbing ripples, clay and silt bands and occasional foreset structures, with the upper exposures exhibiting cut and fill, and dune forms. This is typical of a low energy environment, characterised by fluctuations in the relative importance of suspended sediment rain-out and density underflows (Smith & Ashley, 1985) followed by low energy glaciofluvial accretion across the infilled lake-floor. The absence of rimmed mounds and the thickness of the deposits imply that the ice walled lake plains formed in a stable environment with a large supraglacial debris cover and slow rates of ablation (cf. Clayton *et al.*, 2008). The lack of well developed foreset structures at Faugh sand pit and the variously orientated dune forms suggests that supraglacial drainage, at this location, was both transient and in a state of flux. Modern analogues in Iceland reveal the prevalence of such ice-walled lakes within ice-cored kame terraces and proglacial outwash (Fig. 15a, b, c & d).

The centres of the flat-topped hills are relatively undisturbed with faulting generally limited to small, centimetre scale faults and folds (e.g. LFA F1 & 2). This indicates that the ice was perforated almost to the glacier substrate (Dyke & Evans 2003). The marginal zones, in contrast (e.g. LFA F3), are heavily disturbed, as indicated by major debris flow deposits, large scale faulting and interbedded diamicton and stratified units (Eyles, 1979; Eyles *et al.*, 1987; Mager & Fitzsimons, 2007) associated with gravity flows into the lake and vertical collapse following the removal of the ice walls. The geomorphology shows evidence for some small kettle-holed features within the flat-topped hills. This is consistent with an ice-walled model of deposition (e.g. Clayton & Cherry, 1967; Clayton *et al.*, 2008). Flat-topped hills occupy the central tract of the kame belt, often occurring in juxtaposition and linked by series of discontinuous ridges, attesting to their origin as infilled collapsed tunnel systems in a well developed glacier karst (Clayton, 1964).

The kame belt is implicitly associated with a complex meltwater drainage system, situated both to the north and the south of the glaciofluvial complex. South of the kame belt, along the Pennine escarpment, the meltwater network is dominated by obliquely (SE-NW) cutting, anastomising subglacial channels with undulatory long profiles (Type 1). Further up the flank of the Pennine escarpment are a series of short lateral channels (Type 2) at heights of between 330-420 m demarcating the positions of the ice margin during downwasting (Dyke, 1993; Hätterstrand, 1998). Water is transferred into the subglacial network via a series of subglacial chutes (Type 3) which are deeply incised down slope at right angles to the lateral channels (e.g. Sissons, 1960, 1961; Russell, 1995; Glasser & Sambrook Smith, 1999). These subglacial chutes can be reconciled with a polythermal ice margin. The lateral channels formed during periods when the ice margin was cold-based, and then, when warm-bedded conditions developed, water was transferred down into the subglacial drainage network via these chutes, possibly on a seasonal cycle (cf. Sissons, 1961). This meltwater system infringes upon the southern-most margin of the

kame belt resulting in the dissection of the glaciofluvial deposits into elongate erosional remnants by meltwater channels. The Eden Valley, which is deeply incised into Permo-Triassic sandstone, could potentially have been a tunnel valley, capable of transporting significant amounts of sediment into the kame belt. This tentative conclusion is based on the alignment of many meltwater channels on the Pennine escarpment, which trend towards the current River Eden (Fig. 5), and the south-western arm of the kame belt which trends out of the Eden Valley (Fig. 5). Meltwater also entered the Brampton kame belt from off the Penrith sandstone escarpment, with several flights of small channels cutting across the ridge (Livingstone *et al.*, 2008).

A major subglacial meltwater channel sourced from the Hallbankgate esker cuts through the Irthing-South Tyne watershed into the Tyne Valley drainage system in the northern-most zone of the kame belt. This could either have acted as a proglacial over-spill channel from water running through the kame belt and therefore a time transgressive relict of subglacial flow across the watershed, or it could relate to active subglacial flow across the watershed as part of a major ice drainage network. Its undulatory nature suggests the latter (Paterson, 1994).

Model of formation for the Brampton kame belt

The Brampton kame belt is envisaged to have formed in an ice-contact meltwater drainage network that evolved spatially and temporally from a sub-marginal and subglacial system to a progressively supraglacial system through the enlargement of a complex glacier karst (*sensu* Clayton, 1964) (Fig. 16).

The presence of an extensive subglacial meltwater system leading into (Pennine escarpment & Eden Valley) and out of (Hallbankgate meltwater channel) the kame belt suggests that initial drainage was subglacial, as part of a combined Vale of Eden-Tyne Gap drainage network (Livingstone *et al., submitted manuscript*). However, as ice from both Scotland and the Lake District retreated westwards back across the Tyne Gap (Trotter, 1929, Livingstone, *et al., submitted manuscript*) ice downwasted and stagnated within the lee of the Pennine escarpment and Penrith sandstone outcrop (rising up to 260 m O.D.), both of which probably acted as pinning points (e.g. Ó Cofaigh *et al.*, 1999). Hence, initial deposition of the kame belt likely involved subglacial esker development (Brennand, 2000) (Fig. 16). Esker sedimentation would have been driven by confluent meltwater, the presence of abundant sediment eroded from the Permo-Triassic sandstone and compressive flow and stagnation of ice against the reverse slope of the Tyne Gap (cf. Punkari, 1997, Mäkinen, 2003). Some of the higher and longer eskers, which often lead into the meltwater channels, such as the Hallbankgate esker, Brampton ridge and the S-N orientated esker trending out of the Eden Valley (Fig. 5), are likely examples of these subglacial features. Cyclical sedimentation and fining outwards corresponds to a variable discharge regime, with the marginal-subglacial meltwater associations along the Pennine escarpment able to facilitate rapid seasonal changes of meltwater flow into the subglacial network (Sissons, 1961; Brennand & Shaw, 1996; Mäkinen, 2003).

As the ice continued to stagnate and downwaste the early phase of esker sedimentation evolved into a complex 'glaciofluvial moraine' similar to many interlobate areas (e.g. Warren & Ashley,

1994; Brennand & Shaw, 1996; Thomas & Montague, 1997; Punkari, 1997; Mäkinen, 2003; Russell *et al*., 2003; Sharp *et al*., 2007). This evolution led to the progressive development of glacial karst (Fig. 16), with perforation of ice occurring by strain softening, tunnel collapse, crevasse formation, and supra/englacial meltwater drainage (e.g. Clayton, 1964).

Open channel, supraglacial streams (Fig. 16) flowing along the ice surface and constrained laterally by ice walls (e.g. Warren & Ashley, 1994; Bennett & Glasser, 1996) underwent successive phases of capture and abandonment (cf. Thomas & Montague, 1997), resulting in the development of complex braided networks of subdued, discontinuous ridges (Price, 1966, 1969, 1973; Gustavson & Boothroyd, 1987; Huddart, 1999). Sediment architecture reveals glaciofluvial deposits typical of modern braided stream deposits, (e.g. Miall, 1977, 1985) thus attesting to this model of formation. Englacial sedimentation and the development of sub-aerial ice-walled conduits following tunnel roof collapse are also likely to have developed as the ice downwasted (Huddart, 1999) (Fig. 16). As successive stages of topographic inversion occurred multiple changes in drainage configuration could have led to the eventual development of a broad, shallow supraglacial trough as observed at Vegbreen, Svalbard (Huddart, 1999) thus accounting for the extensive sweep of continuously deposited glaciofluvial deposits (Fig. 16).

The genesis of ice-walled lakes occurred at a late stage in the development of the kame belt (Fig. 16). The lack of faults within the central portion of the flat-topped hill and the fact that they often overlaid ridges supports the notion that the lakes were perforated right down to the glacial substrate (Dyke & Evans, 2003). Therefore, the kame belt was thought to be initially dominated by subglacial and then englacial-supraglacial meltwater drainage networks which probably exited via the Hallbankgate meltwater channel, thus preventing the development of a lake against the reverse slope of the Tyne Gap, as is typical of many esker complexes (e.g. Banerjee & McDonald, 1975; Gorrell & Shaw, 1991; Brennand, 1994; Mäkinen, 2003). As the ice continued to downwaste and stagnate a thin, chaotic, dead ice-cored apron developed, which prevented the effective discharge of meltwater, therefore causing ponding either in collapsed subglacial tunnels (Clayton, 1964), or via the expansion of supraglacial lakes into ice-walled lakes due to basal melting (Smed, 1962; Johnson & Clayton, 2003; Clayton *et al*., 2008). During this stage topographic inversion resulted in the extensive reworking of sediments by debris flows, water escape and vertical collapse. This late-stage chaotic model of supraglacial outwash deposition, lake development, sediment re-distribution and meltwater drainage is epitomised by the multitude of palaeo-currents exhibited within the upper-most sediments.

These final stages in the evolution of the kame belt would have likely involved glaciofluvial supraglacial outwash extending out across the dead-ice cored apron (Rich 1943; Price 1969; Thomas et al., 1985; Gustavson & Boothroyd, 1987; Evans, 2009), leading to the development of hummocky, chaotic, kettle-holed terrain (e.g. Cook, 1946; Clayton, 1964) (Fig. 15 & 16). Spatially this is consistent with the topography of the kame belt, whereby the northern and central zones exhibit striking linearity characterised by the partial preservation of the drainage network despite topographic inversion (Price, 1969; Evans & Twigg, 2002). Conversely, the south-eastern corner exhibits a chaotic kame and kettle landscape, with little evidence of linearity. This is more akin to a thick, extensive deposition of supraglacial 'pitted' outwash during a later stage of

evolution, and on-top of relatively thick ice (Rich 1943; Price 1969; Thomas et al., 1985; Gustavson & Boothroyd, 1987).

The lack of well developed meltwater channels within the kame belt itself indicates that ice-marginal and proglacial meltwater drainage must have shifted direction during the latter stages of ice recession. South of the Penrith sandstone outcrop the Pennine escarpment meltwater network exhibits a time-transgressive morphology, with channels running parallel to each other at successively lower elevations and trending towards the Eden Valley. Thus at some point during deglaciation as the active margin stagnated within the Penrith sandstone outcrop (Trotter, 1929; Livingstone *et al*., 2008) the Pennine escarpment meltwater input into the kame belt must have been severed.

Conclusions:

The Brampton kame belt demonstrates a complex mode of deglacial deposition involving both esker and kame forms/processes (Fig. 16) caused by ice stagnating and downwasting in the lee of the Penrith sandstone ridge and north Pennine escarpment. It is composed of flat-topped hills, ridges and depressions, interpreted as ice-walled lake plains, ice-contact meltwater drainage networks and kettle holes respectively. Sedimentation evolved both spatially and temporally from a sub-marginal and sub-glacial drainage system through the enlargement of a complex glacio-karst. This led to the development of englacial and supraglacial drainage systems within the ice-cored terrain, with ponding leading to the development of ice-walled lakes. Topographic inversion led to the distinctive suite of landforms and represents an end product of a depositional landscape similar to those currently forming at many modern glacier margins (Fig. 15). The Brampton kame belt formed during deglaciation, when ice, which was previously converging on the Tyne Gap from Scotland and the Lake District, began to retreat westwards back across the Irthing-Tyne watershed. Further retreat led to the formation of Lake Carlisle and the stagnation of ice within the Penrith sandstone outcrop.

Based on the model presented in this paper (Fig. 16) a number of general conclusions can be drawn regarding the formation of kame belts:

1. We propose that kame belts demonstrate not only a polygenetic topography (e.g. ridges, flat-topped hills and depressions) but also a time-transgressive evolution with sedimentation controlled primarily by an enlarging glacier karst. The Brampton kame belt demonstrates the potential importance of dead-ice development and an evolving glacier karst in the formation of glaciofluvial depo-centres as it provides a mechanism for both triggering and promoting extensive sedimentation within the ice in various ice-walled settings.

2. Kame formation is shown to be very dynamic, with downwasting, debris flows, melt-out of dead-ice and enlargement of the glacier karst all leading to a shifting glaciofluvial network characterised by both constrained and unconstrained flow, en- sub- and supra-glacial drainage, and ponding. This dynamism explains the complex poly-phase and polygenetic geomorphology and sedimentology exhibited within kame belts.

3. By their very nature kame belts are associated with meltwater drainage of the ice mass and therefore should not be treated in isolation of other glaciofluvial and glaciolacustrine landforms with which they are inextricably linked in a spatial and temporal continuum.

Acknowledgments:

References

Aitken, J. F., (1995). Lithofacies and depositional history of a Late Devensian ice-contact deltaic complex, northeast Scotland. *Sedimentary Geology,* 99; 111-130.

Allen, J. R. L. (1968). Current Ripples. *North-Holland, Amsterdam*, 433 pp

Allen, J.R.L., (1973). A classification of climbing-ripple cross-lamination. *Journal of the Geological Society*, 129(5); 537-541.

Allen, J.R.L., (1984). Sedimentary Structures - their Character and Physical Basis. Elsevier, Amsterdam.

Arthurton, R. S. & Wadge, A. J. (1981). Geology of the country around Penrith. *Memoir of the British Geological Survey, HMSO, London.*

Ashley, G. M., Southard, J. B. and Boothroyd, J. C. (1982). Deposition of climbing-ripple beds: a flume simulation. *Sedimentology*, 29; 67-79.

Banerjee, I. & McDonald, B. C., (1975). Nature of esker sedimentation. *In*, Jopling, A. V. and McDonald, B. C. *Glaciofluvial and glaciolacustrine sedimentation. Society of Economic Paleontologists and Mineralogists Special Publication No. 23.*

Benn, D. I. & Evans, D. J. A., (1998). Glaciers and Glaciation. Edward Arnold, London.

Bennett, M. & Glasser, N. (1996). Glacial Geology: Ice Sheets and Landforms. Wiley, Chichester.

Boothroyd, J. C. & Ashley, G. M. (1975). Processes, bar morphology, and sedimentary structures on braided outwash fans, northeastern Gulf of Alaska. *In*, Jopling, A. V. and McDonald, B. C. *Glaciofluvial and glaciolacustrine sedimentation. Society of Economic Paleontologists and Mineralogists Special Publication No. 23.*

Boulton, G. S., (1967). The development of a complex supraglacial moraine at the margin of Sørbreen, Ny Friesland, Vestspitsbergen. *Journal of Glaciology* 6; 717–735.

Boulton, G. S., (1972). Modern Arctic glaciers as depositional models for former ice sheets. *Journal of the Geological Society of London,* 128; 361-393.

Brennand, T. A. (1994). Macroforms, large bedforms and rhythmic sedimentary sequences in subglacial eskers, south-central Ontario: implications for esker genesis and meltwater regime. Sedimentary Geology, 91; 9-55.

Brennand, T. A. & Shaw, J. (1996). The Harricana glaciofluvial complex, Abitibi region, Quebec: its genesis and implications for meltwater regime and ice sheet dynamics. Sedimentary Geology, 102; 221-262.

Brennand, T. A. (2000). Deglacial meltwater drainage and glaciodynamics: inferencesfrom Laurentide eskers, Canada. *Geomorphology*, 32; 263-293.

Brodzikowski, K. and van Loon, A. J., (1991). Glacigenic sediments.

Cheel, R. J. & Rust, B. R. (1982). Coarse-grained facies of glaeiomarine deposits near Ottawa, Canada. In: Davidson-Arnott, R. Nickling W. and Fahey, B.C. (Eds), *6th Guelph Symposium on GeomorphologyResearch in Glacial, Glacio-fluvial, and Glacio-lacustrine Systems*, GeoBooks, Norwich, pp. 279–295.

Clark, C. D., Evans, D. J. A., Khatwa, A., Bradwell, T., Jordan, C. J., Marsh, S. H., Mitchell, W. A. and Bateman, M. D., (2004). Map and GIS database of glacial landforms and features relating to the last British ice Sheet. *Boreas,* 33; 359-375.

Clayton, L. (1964). Karst topography on stagnant glaciers. *Journal of Glaciology,* 5; 107–112.

Clayton, L. & Cherry, J. A. (1967). Pleistocene superglacial and ice-walled lakes of west-central North America. *North Dekota Geological Survey, Miscellaneous Series,* 30; 47–52.

Clayton L., Attig J.W., Ham N.R., Johnson M.D., Jennings C.E. & Syverson K.M. (2008). Ice-walled-lake plains: implications for the origin of hummocky glacial topography in middle North America. *Geomorphology* 97, 237-248.

Collinson, J. D., (1996). Alluvial Sediments. *In*, Reading, H. G. (ed). *Sedimentary environments: processes, facies and stratigraphy.*

Collinson, J. D. & Thompson, D. B. (1989). Sedimentary Structures. *Unwin Hyman, London.*

Cook, J. H. (1946). Kame-complexes and perforation deposits. *American Journal of Science*, 24; 573-583.

Donnelly, R. and Harris, C., (1989). Sedimentology and origin of deposits from a small ice-dammed Lake. Leirbreen, Norway. *Sedimentology*, 36; 581-600.

Dyke, A. S. (1993). Landscapes of cold-centred LateWisconsinan ice caps, Arctic Canada. *Progress in Physical Geography*. 17; 223–247.

Dyke, A. S. & Evans, D. J. A., (2003). Ice-marginal terrestrial landsystems: northern Laurentide and Innuitian ice sheet margins. In Evans, D. J. A. (ed.), *Glacial Landsystems*. Arnold, London, 143-165.

Evans, D. J. A. & Twigg, D. R. (2002). The active temperate glacial landsystem: a model based on Breiðamerkurjökull and Fjallsjökull, Iceland. *Quaternary Science Reviews*, 21; 2143-2177.

Evans, D. J. A., Clark, C. D. and Mitchell, W. A., (2005). The last British Ice Sheet: A review of the evidence utilised in the compilation of the Glacial Map of Britain. *Earth Science Reviews,* 70; 253-312.

Evans, D. J. A. (2009). Controlled moraines: origin, characteristics and palaeoglaciological implications. *Quaternary Science Reviews*, 28(3-4); 183-208.

Evans, D. J. A., Livingstone, S. J., Vieli, A. and Ó Cofaigh, C, (2009). The palaeoglaciology of the central sector of the British and Irish Ice Sheet: reconciling glacial geomorphology and preliminary ice sheet modelling. *Quaternary Science Reviews*, 28; 739-757.

Eyles, N. (1979). Facies of supraglacial sedimentation on Icelandic and Alpine temperate glaciers. *Canadian Journal of Earth Science,* 16; 1341–1361.

Eyles, N., Clark, B. M. and Clague, J. J. (1987). Coarse-grained sediment gravity flow facies in a large supraglacial lake. *Sedimentology*, 34; 193-216.

Glasser, N. F. & Sambrook Smith, G. H. (1999). Glacial meltwater erosion of the Mid-Cheshire Ridge: implications for ice dynamics during the Late Devensian glaciation of northwest England. Journal of Quaternary Science, 14; 703-710.

Gravenor, C. P. & Kupsch, W. O., (1959). Ice-distintegration features in western Canada. Journal of Geology, 67; 48-64.

Greenwood S. L., Clark, C. D. and Hughes, A. L. C., (2007). Formalising an inversion methodology for reconstructing ice-sheet retreat patterns from meltwater channels: application to the British Ice Sheet. *Journal of Quaternary Science*, 22(6); 637-645.

Gordon, S., Sharp, M., Hubbard, B., Smart, C., Ketterling, B. & Willis, I. (1998). Seasonal reorganisation of subglacial drainage inferred from measurements in boreholes. *Hydrological Processes*, 12; 105-133.

Gorrell, G. & Shaw, J. (1991). Deposition in an esker, bead and fan complex, Lanark, Ontario, Canada. *Sedimentary Geology*, 72; 285-314.

Gustavson, T. C. & Boothroyd, J. C. (1987). Depositional model for outwash, sediment sources, and hydrologic characteristics, Malaspina Glacier, Alaska: A modern analog of the southeastern margin of the Laurentide Ice Sheet. *Geological Society of America*, 99(2); 187-200.

Ham, N. R. & Attig, J. W., (1997). Pleistocene geology of Lincoln County, Wisconsin, *Wisconsin Geological and Natural History Survey Bulletin* 93, 31 pp.

Hättestrand, C. (1998). The glacial geomorphology of central and northern Sweden. *Sveriges Geologiska Undersökning Ca,* 85; 1–47.

Holmes, C. D. (1947). Kames. *American journal of Science*, 245; 240-249.

Huddart, D. (1970). Aspects of glacial sedimentation in the Cumberland Lowland. *Unpublished PhD Thesis*.

Huddart, D. & Bennett, M. R., (1997). The Carstairs Kames (Lanarkshire, Scotland): morphology, sedimentology and formation. *Journal of Quaternary Science,* 12(6); 467-484.

Huddart, D. (1981). Fluvioglacial systems in Edenside (middle Eden Valley and Brampton kame belt). In, Boardman J. (ed), *Eastern Cumbria – Field Guide*. Quaternary Research Association, London, 81-103.

Huddart, D., Bennett, M. R. and Glasser, N. F., (1999). Morphology and sedimentology of a high-arctic esker system: Vegbreen, Svalbard. *Boreas*, 28; 253-273.

Jackson, I., (1979). The sand and gravel resources of the country around Brampton, Cumbria: description of 1:25,000 resources sheet NY 55 and part of NY 56. *Mineral Assessment Report for the Institute of Geological Sciences,* No. 45.

Johnson, M. D. & Clayton, L. (2003). Supraglacial landsystems in lowland terrain. In Evans, D. J. A. (ed). *Glacial Landsystems.* Arnold, London, pp. 228-258.

Jopling, A. V. & Walker, R. G., (1968). Morphology and origins of ripple-drift cross lamination, with examples from the Pleistocene of Massachusetts. *Journal of Sedimentary Research,* 38(4); 971-984.

Kjaer, K. H. & Krüger, J., (2001). The final phase of dead-ice moraine development: processes and sediment architecture, Kötlujökull, Iceland. *Sedimentology*, 48; 935-952.

Krüger, J. (1994). Glacial processes, sediments, landforms, and stratigraphy in the terminus region of Myrdalsjökull, Iceland. Two interdisciplinary case studies. *Folia Geographica Damica* 21 (1994), pp. 1–233.

Lawson, D. E. (1979). A sedimentological analysis of the western terminus region of the Matanuska Glacier, Alaska. *U.S. Army Cold Regions Research and Engineering Lab. Rpt*. 79-9.

Lawson, D. E. (1981). Distinguishing characteristics of diamictons at the margin of the Matanuska Glacier, Alaska. ANNALS OF Glaciology, 2; 78-83.

Lawson, D. E. (1982). Mobilisation, movement and deposition of active subaerial sediment flows, Matanuska Glacier, Alaska. *Journal of Geology.* 90; 279-200.

Livingstone, S. J., Ó Cofaigh, C. and Evans, D. J. A., (2008). Glacial geomorphology of the central sector of the last British-Irish Ice Sheet. *Journal of Maps*, v2008; 358-377.

Livingstone, S. J., Ó Cofaigh, C. and Evans, D. J. A., (*submitted manuscript*). A major ice drainage pathway of the last British-Irish Ice Sheet: the Tyne Gap, northern England. *Journal of Quaternary Science.*

Mager S. & Fitzsimons S. 2007. Formation of glaciolacustrine Late Pleistocene end moraines in the Tasman Valley, New Zealand. *Quaternary Science Reviews* 26, 743-758.

Mäkinen, J. (2003). Time-transgressive deposits of repeated depositional sequences within interlobate glaciofluvial (esker) sediments in Köyliö, SW Finland. *Sedimentology*, 50; 327-360.

Mair, D. W. F., Sharp, M. J. & Willis, I. C. (2002). Evidence for basal cavity opening from analysis of surface uplift during a high-velocity event: Haut Glacier d'Arolla, Switzerland. *Journal of Glaciology*, 48; 208-216.

McCarroll & Rijsdijk, K. F. (2003). Deformation styles as a key for interpreting glacial depositional environments. *Journal of Quaternary Science,* 18; 473-489.

McDonald, B. C. & Shilts, W. W. (1975). Interpretation of faults in glaciofluvial sediments. In Jopling, A. V. and McDonald, B. C. (eds). *Glaciofluvial and glaciolacustrine sedimentation*, p. 123-131.

McKenzie, G. D., (1969). Observations on a collapsing kame terrace in Glacier Bay National Monument, south-eastern Alaska. *Journal of Glaciology*, 8(54); 413-425.

Miall, A. D., (1977). A review of the braided-river depositional environment. *Earth Science Reviews,* 13; 1-62.

Miall, A. D., (1985). Architectural-element analysis: a new method of facies analysis applied to fluvial deposits. *Earth Science Reviews,* 22; 261-308.

Nemec, W. (1992). Depositional controls on plant growth and peat accumulation in a braidplain delta environment: Helvetiafjellet Formation (Barremian-Aptian), Svalbard. In McCabe, P. J., and Parrish, J. T. (eds). *Controls on the Distribution and Quality of Cretaceous Coals: Boulder, Colorado*, Geomorphological Society of America Special Paper 267.

Ó Cofaigh, C., Lemmen, D. S., Evans, D. J. A. and Bednarski, J. (1999). Glacial landform-sediment assemblages in the Canadian High Arctic and their implications for late Quaternary glaciation. *Annals of Glaciology*, 28; 195-201.

Owen, G., (1997). Origin of an esker-like ridge – erosion or channel fill? Sedimentology of the Monington 'esker' in southwest Wales. *Quaternary Science Reviews*, 16; 675-684.

Paterson, W. S. B. (1994). *The Physics of Glaciers*. Elsevier, Oxford.

Paul, M. A., (1983). Supraglacial landsystem. *In* Eyles N. (eds). *Glacial Geology, 91-90, Pergamon Press, Oxford.*

Price, R. J. (1965). The changing proglacial environment of the Casement Glacier, Glacier Bay, Alaska. *Transactions of the Institute of British Geographers,* 36; 107-116.

Price, R. J., (1966). Eskers near the Casement Glacier, Alaska. *Geografiska Annaler,* 48B; 111-125.

Price, R. J., (1969). Moraines, sandar, kames and eskers near Breidamerkurjokull, Iceland. *Transactions of the Institute of British Geographers,* 46; 17-43.

Price, R. J., (1973). Glacial and fluvio-glacial landforms.

Punkari, M. (1997). Glacial and glaciofluvial deposits in the interlobate areas of the Scandinavian ice sheet. *Quaternary Science Reviews*, 16; 741-753.

Reineck, H. E. & Singh, I. B. (1975). Depositional Sedimentary Environments. Springer Verlag, Berlin.

Rich, J.L. (1943). Buried stagnant ice as a normal product of a progressively retreating glacier in a hilly region. *American Journal of Science,* 241; 95–99.

Ringrose, S. (1982). Depositional processes in the development of eskers in Manitoba. *In* Davidson-Arnott, R., Nickling, W. & Fahey, B. D. (eds): *Research in Glacial, Glaciofluvial and Glacio-Lacustrine Systems*, 117-138. Geobooks, Norwich.

Russell, A. J. (1995). Late Devensian meltwater movement and storage within the Ochil Hills. *Scottish Journal of Geology*, 31, 65–78.

Russell, A. J., Knudsen, Ó., Fay, H., Marren, P. M., Heinz, J. and Tronicke, J., (2001). Morphology and sedimentology of a giant supraglacial, ice-walled, jökulhlaup channel, Skeiðarárjökull, Iceland: implications for esker genesis. *Global and Planetary Change*, 28; 193-216.

Russell, A.J., Fay, H., Marren, P.M., Tweed, F. S. and Knudsen, Ó. (2005). Icelandic jökulhlaup impacts. In: Caseldine, C., Russell, A., Harðardóttir, J. and Knudsen, Ó. (Eds). *Iceland – Modern Processes and Past Environments* vol. 5, Developments in Quaternary Science pp. 153–203.

Russell, A.J., Gregory, A.R., Large, A.R.G., Fleisher P.J. and Harris, T.D. (2007). Tunnel channel formation during the November 1996 Jökulhlaup, Skeiðarárjökull, Iceland, *Annals of Glaciology*, 45; 95–103.

Russell, H. A. J., Arnott, R. W. C. & Sharpe, D. R. (2003). Evidence for rapid sedimentation in a tunnel channel, Oak Ridges Moraine, southern Ontario, Canada. *Sedimentary Geology*, 160; 33-55.

Rust, B. R. (1962). Structure and process in a braided river. *Sedimentology*, 18; 221-245.

Salt, K. E. & Evans, D. J. A., (2004). Superimposed subglacially streamlined landforms of southwest Scotland. *Scottish Geographical Journal,* 120(1+2); 133-147.

Sharpe, D. R., Russell, H. A. J. & Logan, C. (2007). A 3-dimensional geological model of the Oak Ridges Moraine area, Ontario, Canada. *Journal of Maps*, v2007; 239-253.

Shaw, J. (1972). Sedimentation in the ice-contact environment, with examples from Shropshire (England). *Sedimentology*, 18; 23-62.

Sissons, J.B., (1958). Supposed ice-dammed lakes in Britain with particular reference to the Eddleston valley, southern Scotland. *Geografiska Annaler* 40A**;** 159–187.

Sissons, J. B. (1960). Some aspects of glacial drainage channels in Britain. Part I. *Scottish Geographical Magazine*, 76, 131–146.

Sissons, J.B., (1961). Some aspects of glacial drainage channels in Britain. Part II. *Scottish Geographical Magazine*, 77; 15-36.

Smed, P. (1962). Studier over den fynske oguppes glaciale landskabsformer. Meddeleser fra Dansk Geologisk Forening, 15; 1-74.

Smith, N. D. (1985). Proglacial fluvial environment. *In* Ashley, G. M., Shaw, J. and Smith, N. D. (eds). *Glacial Sedimentary Environments.*

Smith, N. D. & Ashley, G. (1985). Proglacial lacustrine environment. *In* Ashley, G. M., Shaw, J. and Smith, N. D. (eds). *Glacial Sedimentary Environments.*

Thomas, G. S. P., Connaughton, M. & Dackombe, R. V. (1985). Facies variation in a Late Pleistocene supraglacial outwash sandur from the isle of Man. *Geological Journal*, 20; 193-213.

Thomas, G. S. P. & Montague, E., (1997). The morphology, stratigraphy and sedimentology of the Carstairs eskers, Scotland, U. K. *Quaternary Science Reviews,* 16; 661-674.

Thomas, G. S. P., Chester, D. K. and Crimes, P. (1998). The Late Devensian glaciation of the eastern Lleyn Peninsula, North Wales: evidence for terrestrial depositional environments. *Journal of Quaternary Science*, 13(3); 255-270.

Trotter, F. M., (1929). The Glaciation of East Edenside, the Alston Block and the Carlisle Plain. *Quarterly Journal of the Geological Society of London,* 85; 549-612.

Trotter, F. M. & Hollingworth, S. E., (1932). The geology of the Brampton district. *Memoir of the Geological Survey of Great Britain*, Sheet 18 (England and Wales).

Warren, W. P. & Ashley, G. M. (1994). Origins of the Ice-contact Stratified Ridges (Eskers) of Ireland. *Journal of Sedimentary Research*, 64A; 433-449.

Williams, P. F. & Rust B. R. (1969). The sedimentology of a braided river. *Journal of Sedimentary Petrology*, 39; 649-679.

Figures:

Figure 1: Topographic map showing the position of the Brampton kame belt within the central sector of the BIIS, and the location of fieldsites and borehole logs
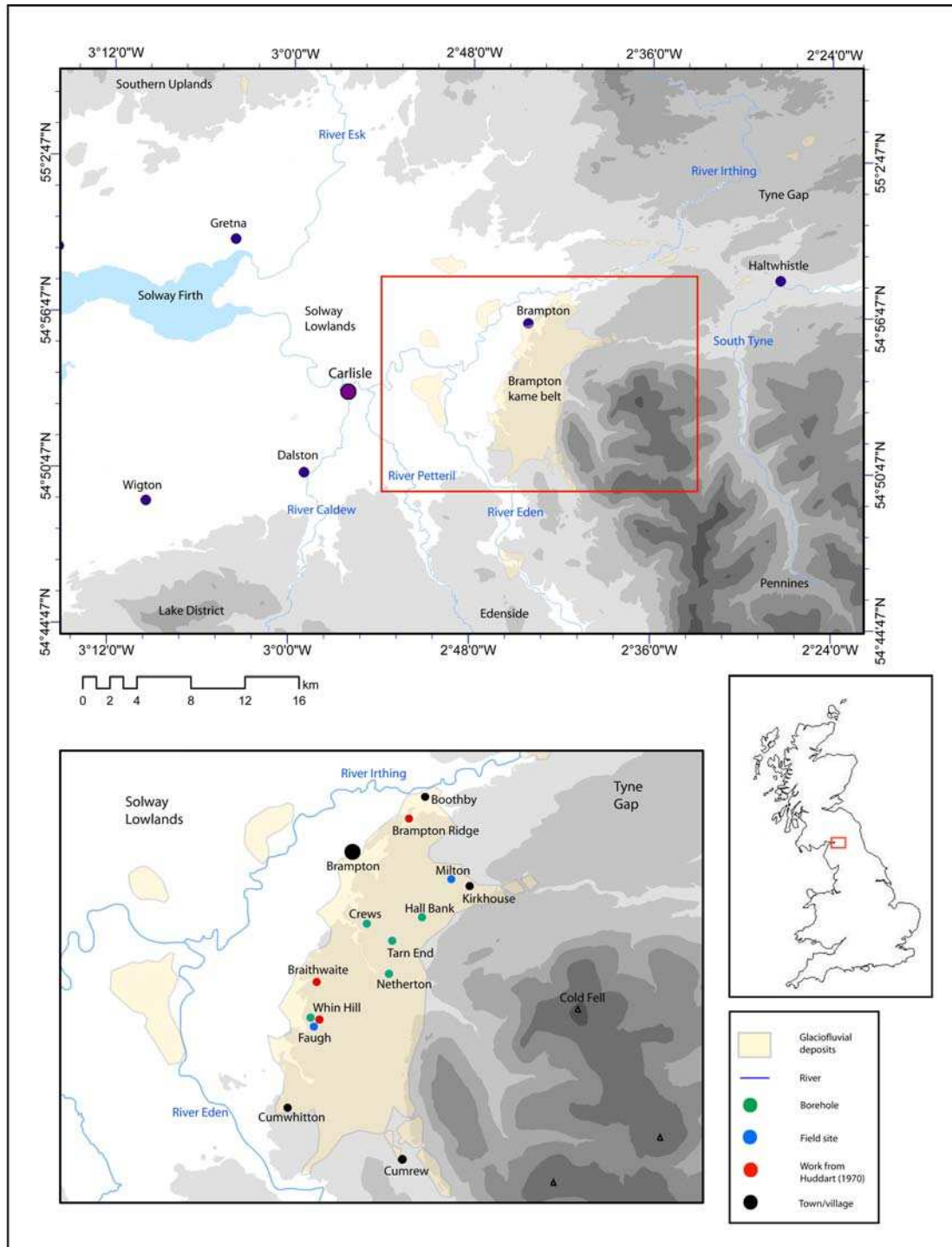
Figure 2: Schematic model for the various types of kames (from Brodzikowski & van Loon, 1991)
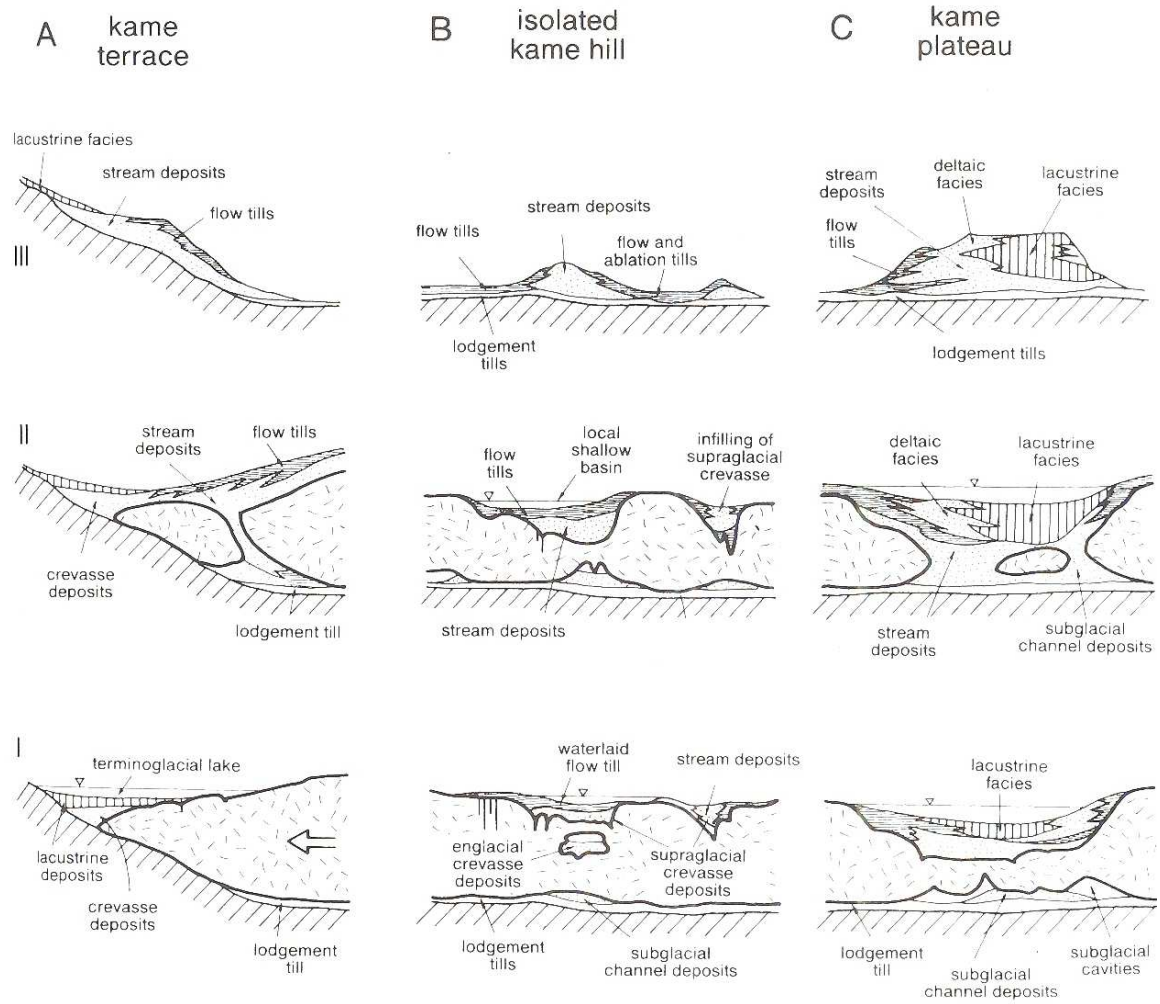
Figure 3: Retreat phenomena in east Edenside demarcating a series of ice marginal positions from the kame belt and meltwater channels (from Trotter, 1929)
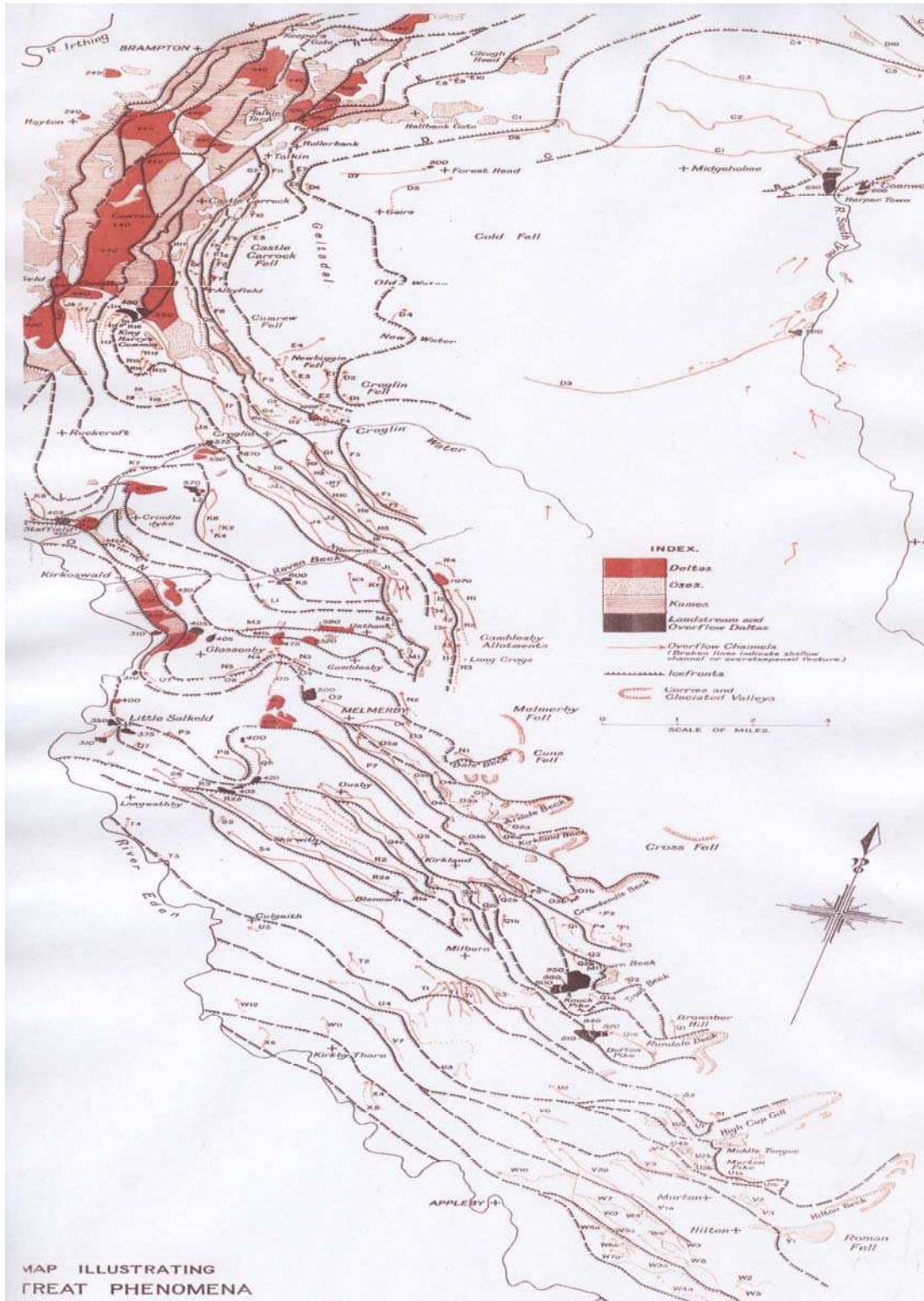
Figure 4: Meltwater channels along the Pennine escarpment and within the Penrith sandstone outcrop (from Arthurton & Wadge, 1981)
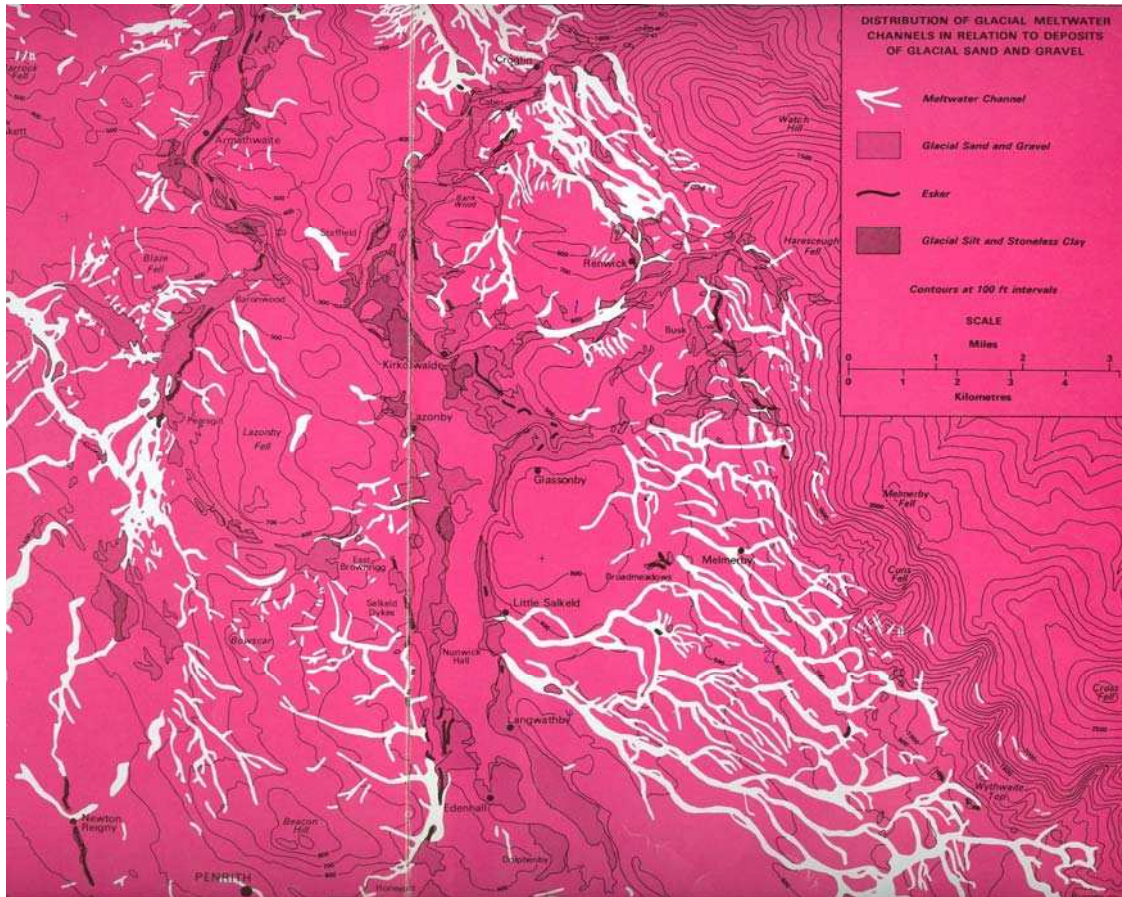
Figure 5: (a) The glacial geomorphology of the Brampton kame belt and surrounding area. Glaciofluvial deposits and meltwater channels have been mapped; (b) 3D NEXTMap DEM of the Brampton kame belt; (c) NEXTMap image of the Brampton kame belt; and (d) Glaciofluvial deposits, flat-topped hills, ridges and meltwater channels mapped from image (c). (*NEXTMap Britain data from Intermap technologies Inc were provided courtesy of NERC via the NERC Earth Observation Data Centre*)

34
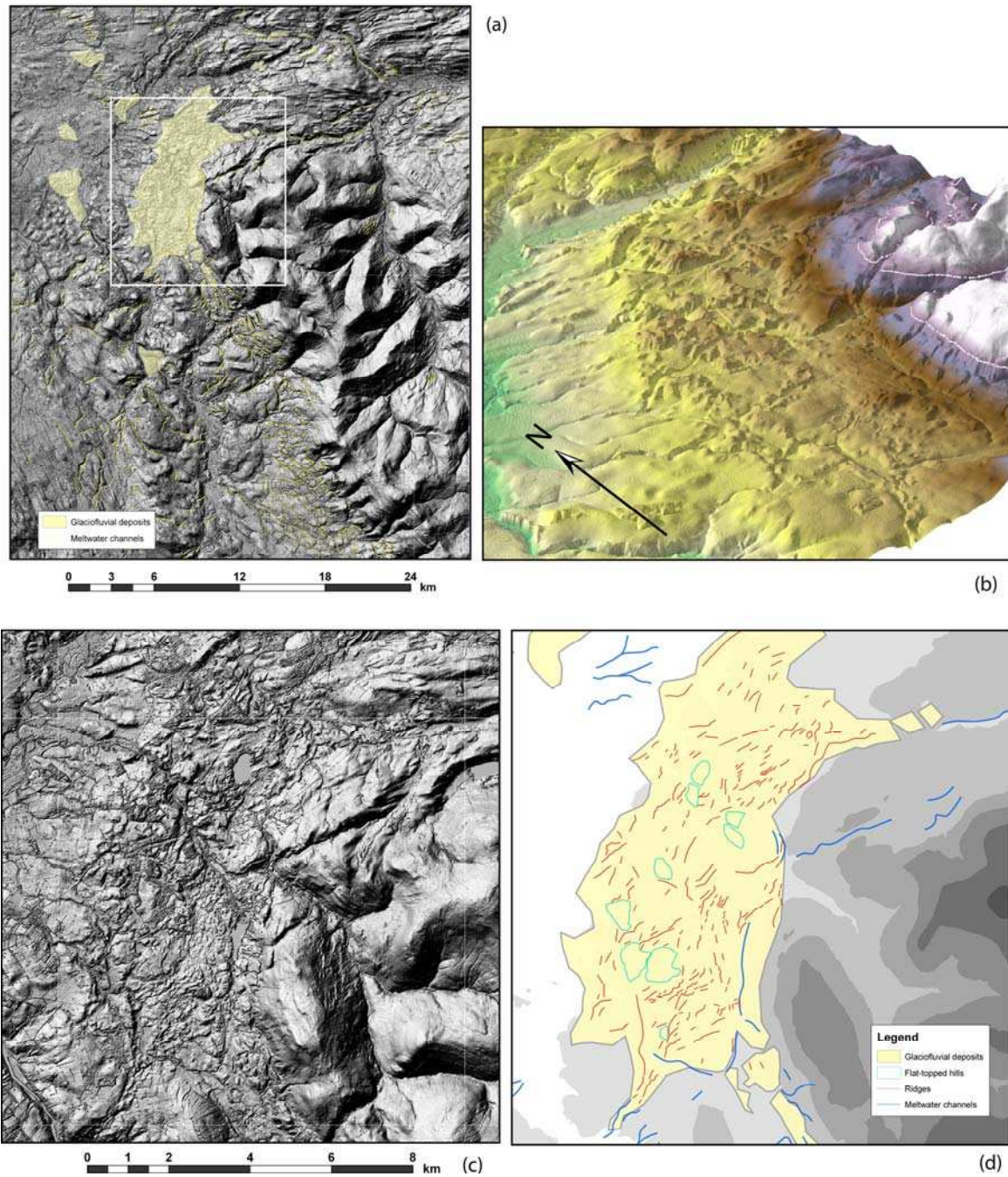
Figure 6: (a) Aerial photographs (Cambridge University) through the northern sector of the Brampton kame belt revealing a series of depressions, meltwater channels, ridges and flat-topped

hills; (b) oblique aerial photograph (Cambridge University) looking north-west along the edge of Talkin Tarn, revealing a series of subdued ridges (marked x).
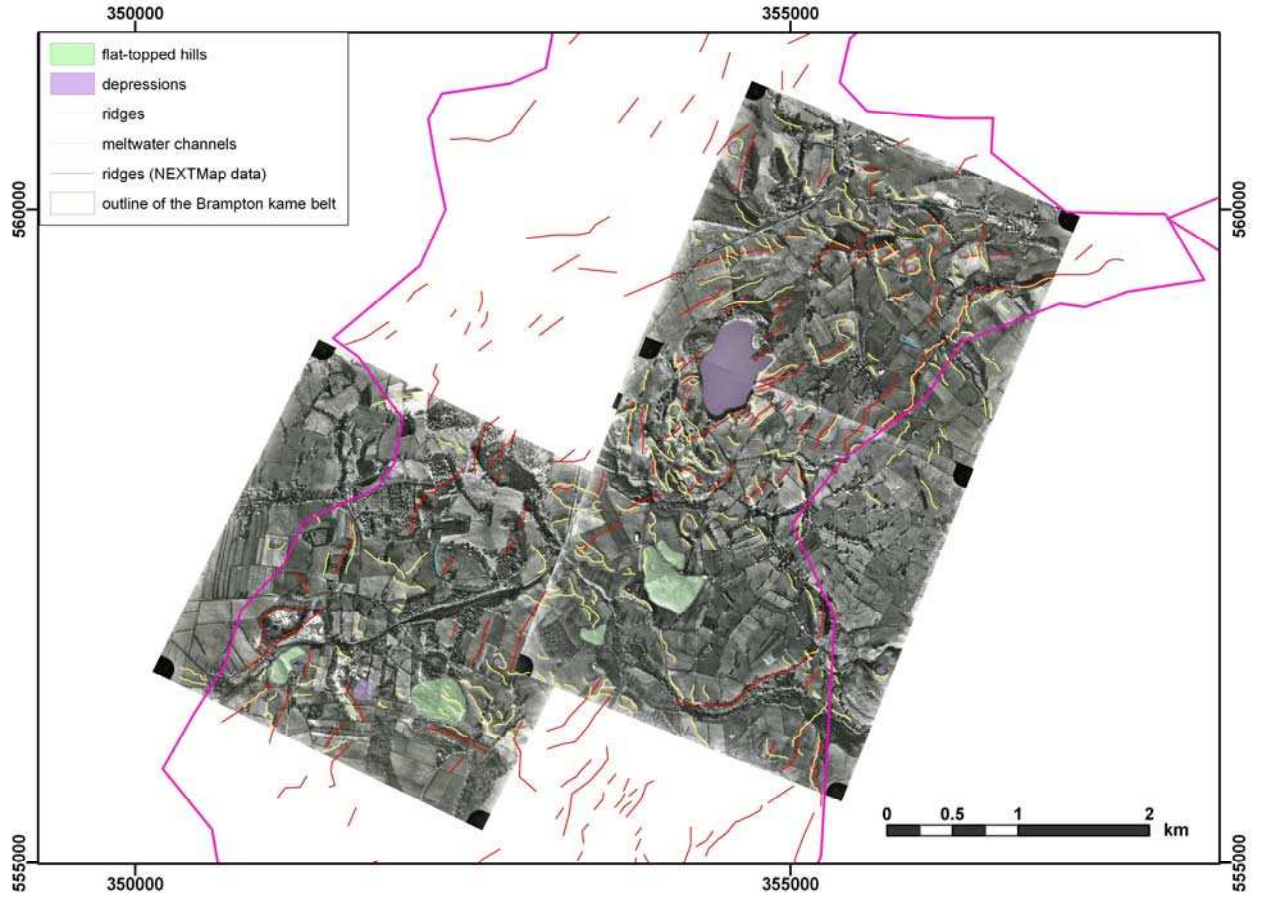
Figure 7: (a) Long-profiles down a network of meltwater channels between Cumrew and Renwick. Note the undulatory profiles in many of them, variable lengths and sudden increases in gradient demarcating the start of Type 3 channels. The channels have been plotted on to an OS map displaying the general SW-NE orientation of the channels, which cut both obliquely and parallel to the Pennine escarpment; (b) Field mapping of 30 meltwater channels between Melmerby and Hartside allowed channels to be subdivided into 3 main types; (c) photograph showing a typical Type 3 channel; and (d) photograph showing a network of Type 1 channels (numbers refer to channel profiling methodology)
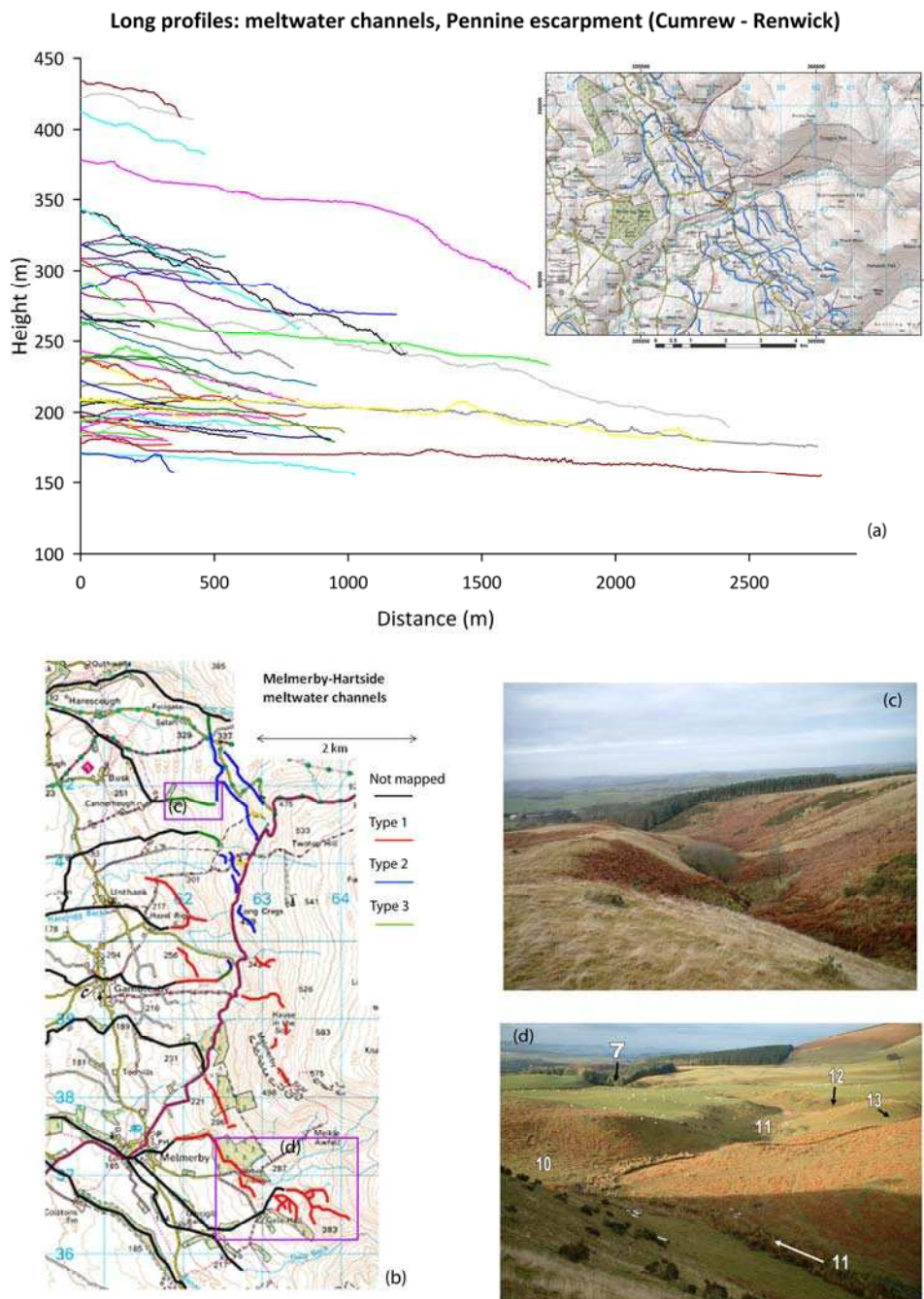
Figure 8: Stratigraphic logs: Kirkhampton sand pit
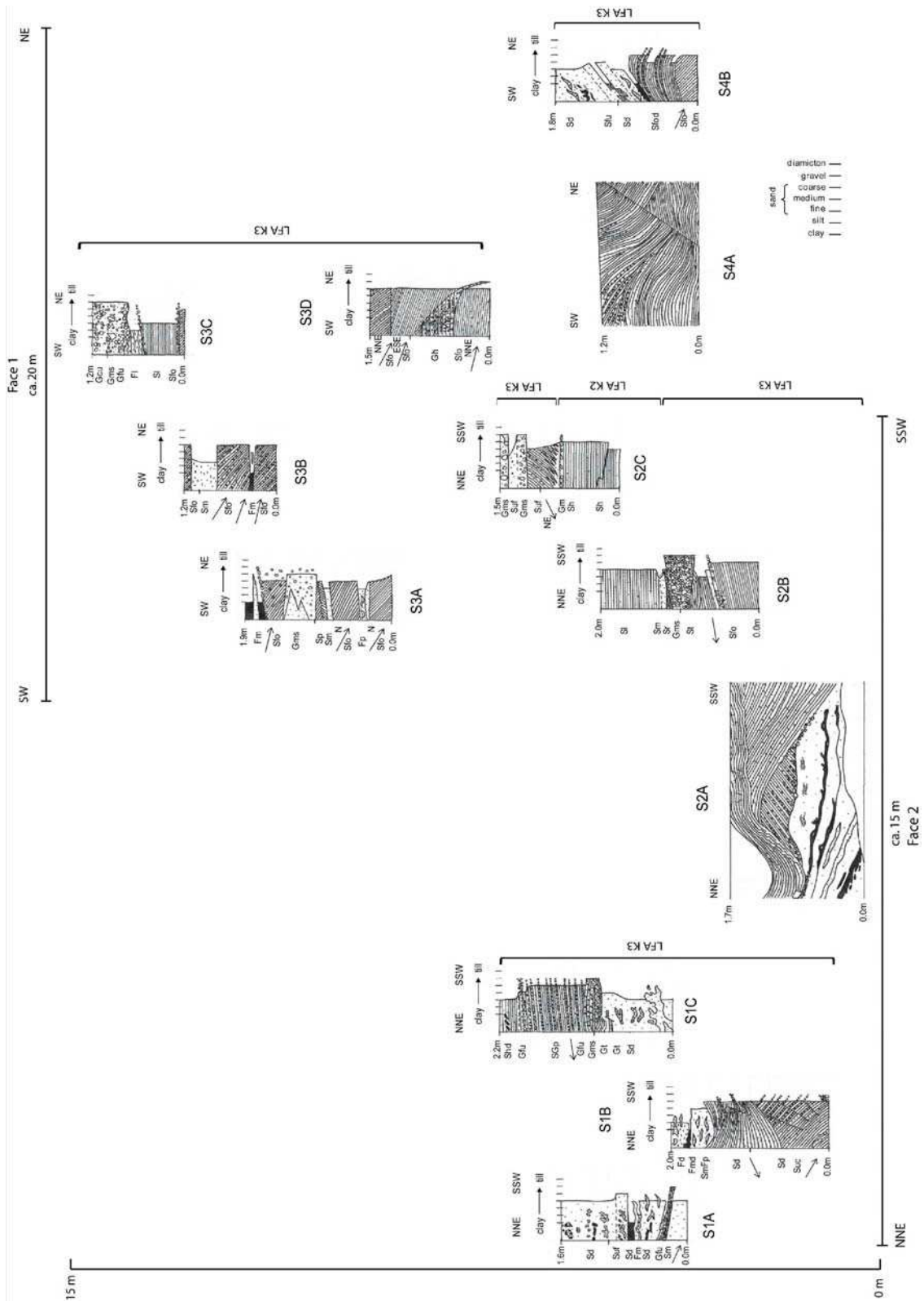
Figure 9: Photographs from Kirkhampton sand pit: (a) LFA K1: tabular cross-beds and planar beds of fine-coarse sand and a couple of trough cross-beds comprised of stratified coarse sand and granule gravel; (b) LFA K1: scour trough cut into parallel laminated sand and comprised of stratified sand and granule gravel with some pebble gravel at the base; (c) LFA K2: thin alternating lithofacies of planar laminated fine sand, fine-grained sinusoidal drapes and type 'A' climbing ripples; (d) LFA K3: tabular cross-bedded sand, stratified coarse sand and granule gravel, massive coarse sand and fine-grained drapes; and (e) vertical collapse structure.
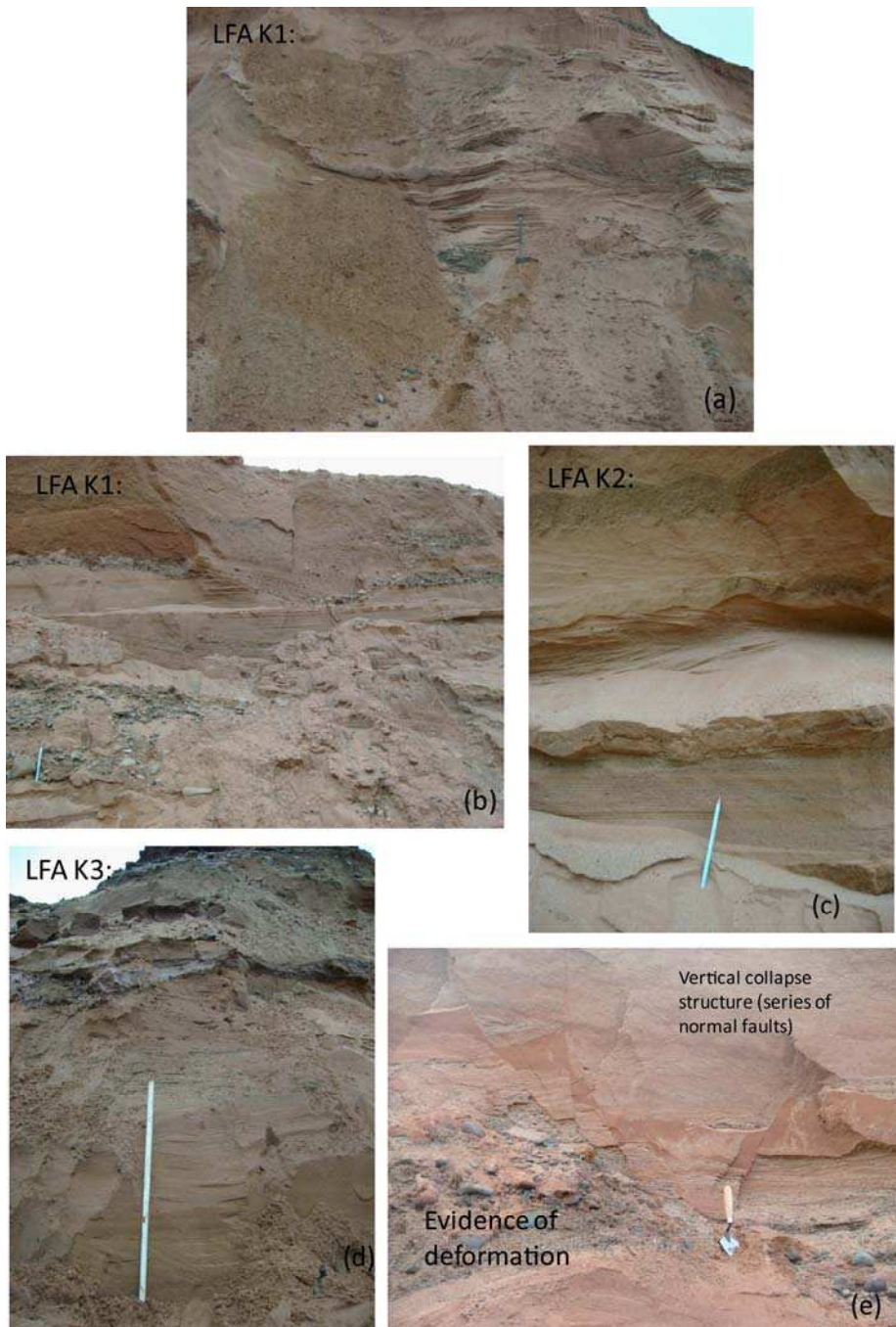
Figure 10: Stratigraphic logs: Brampton ridge sand pit (reproduced from Huddart, 1970)
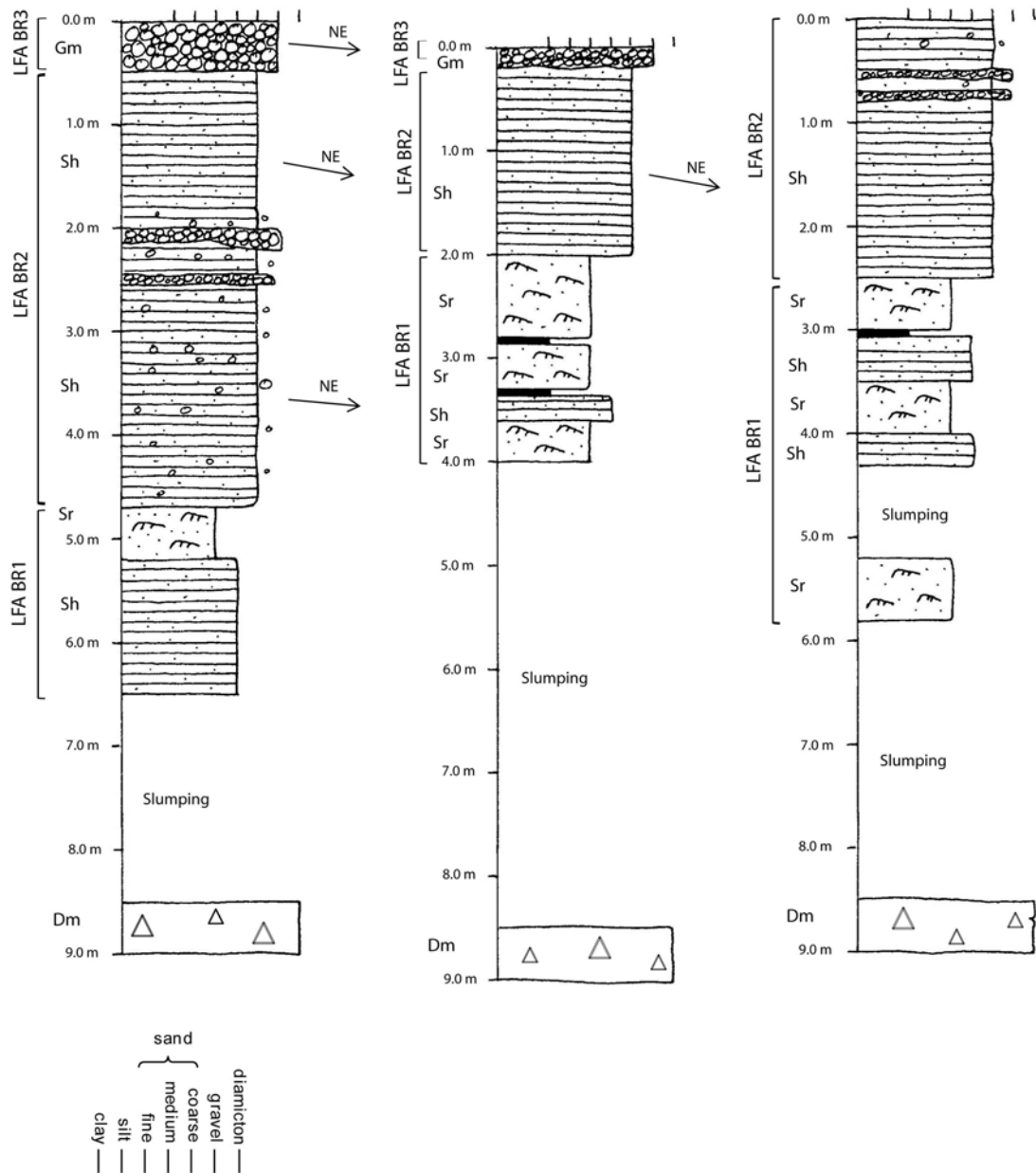
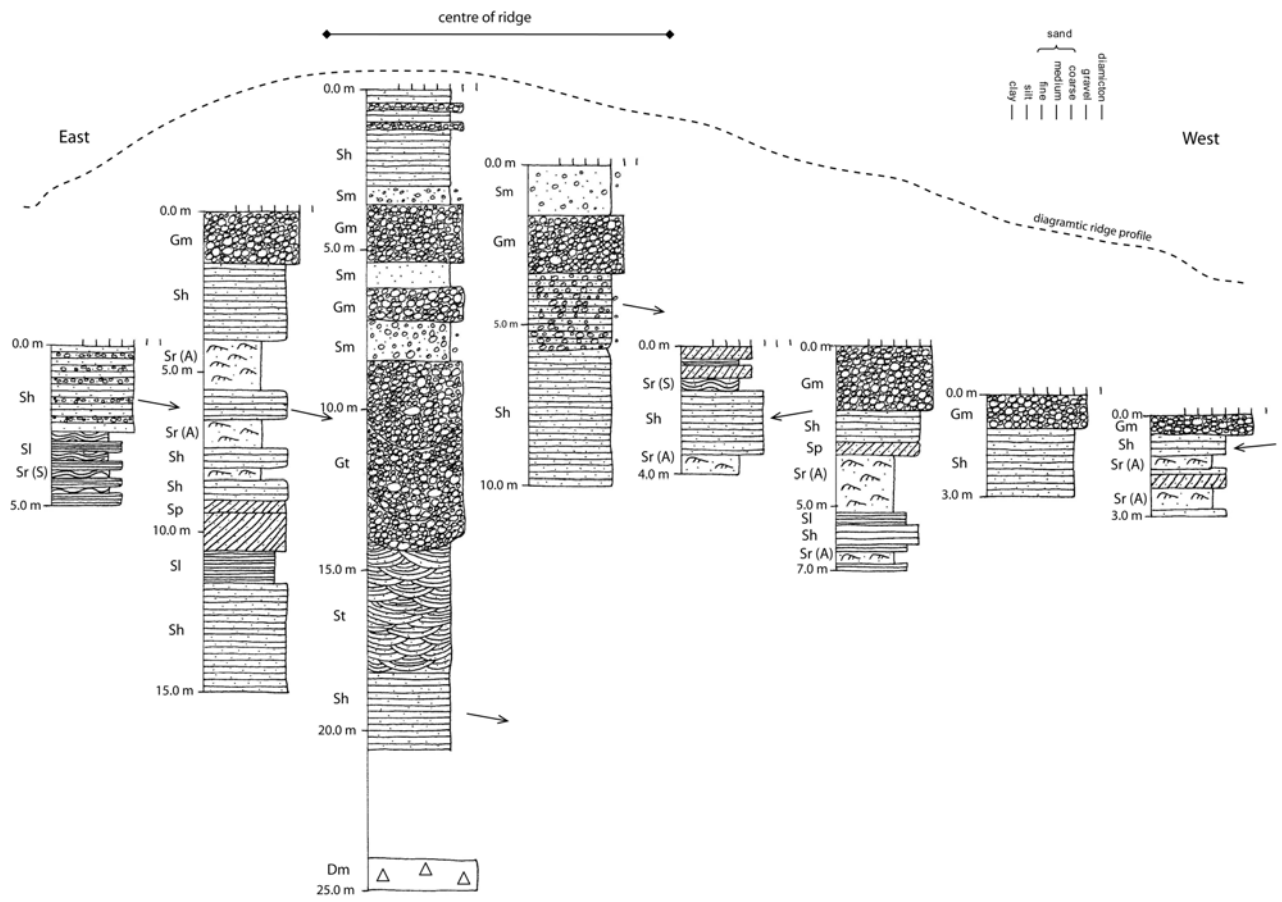*Figure 11:* Stratigraphic logs: Braithwaite's sand pit (reproduced from Huddart, 1970)

Figure 12: Borehole logs through several ridges and flat-topped hills, reproduced from Jackson (1979)
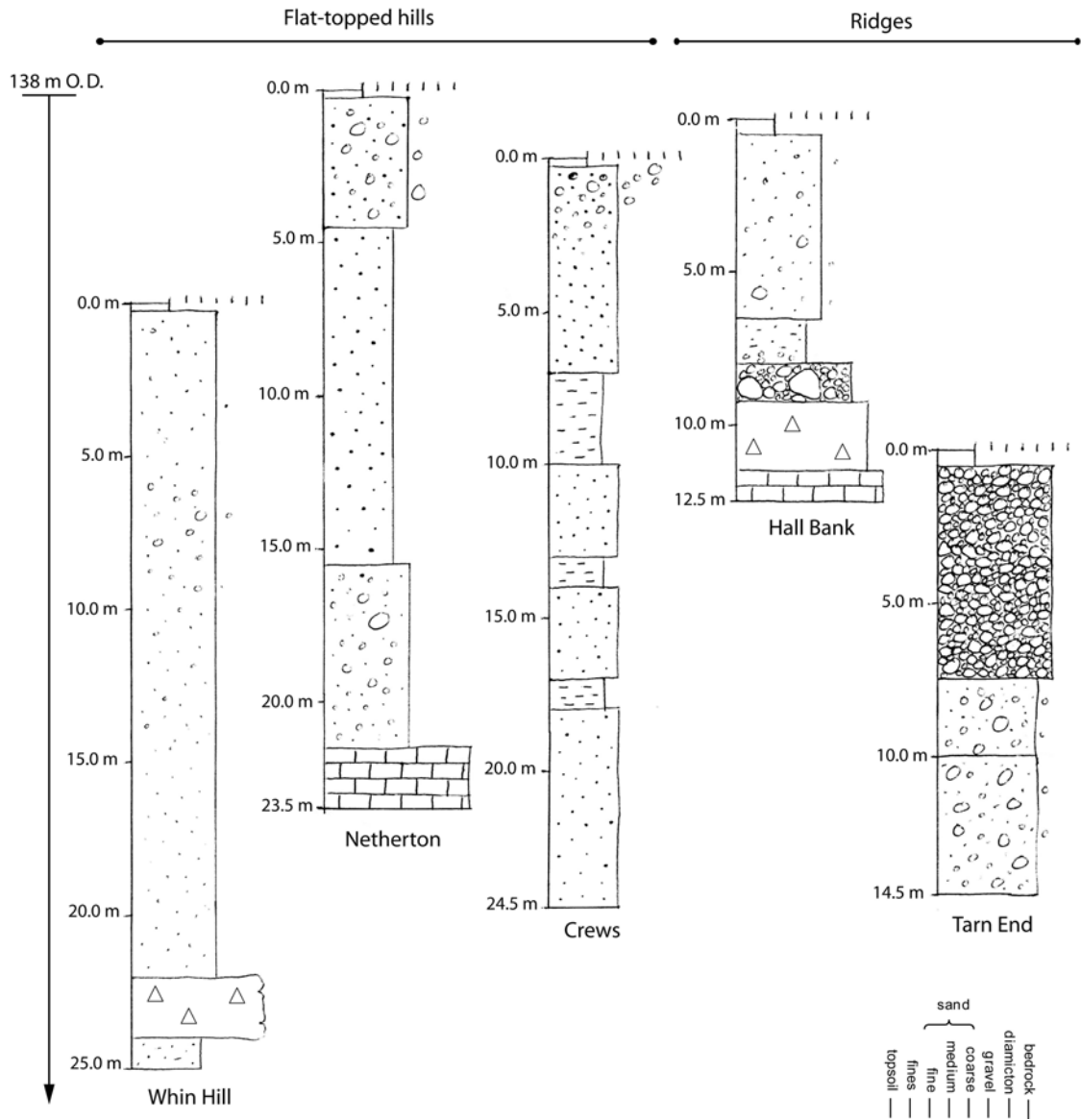
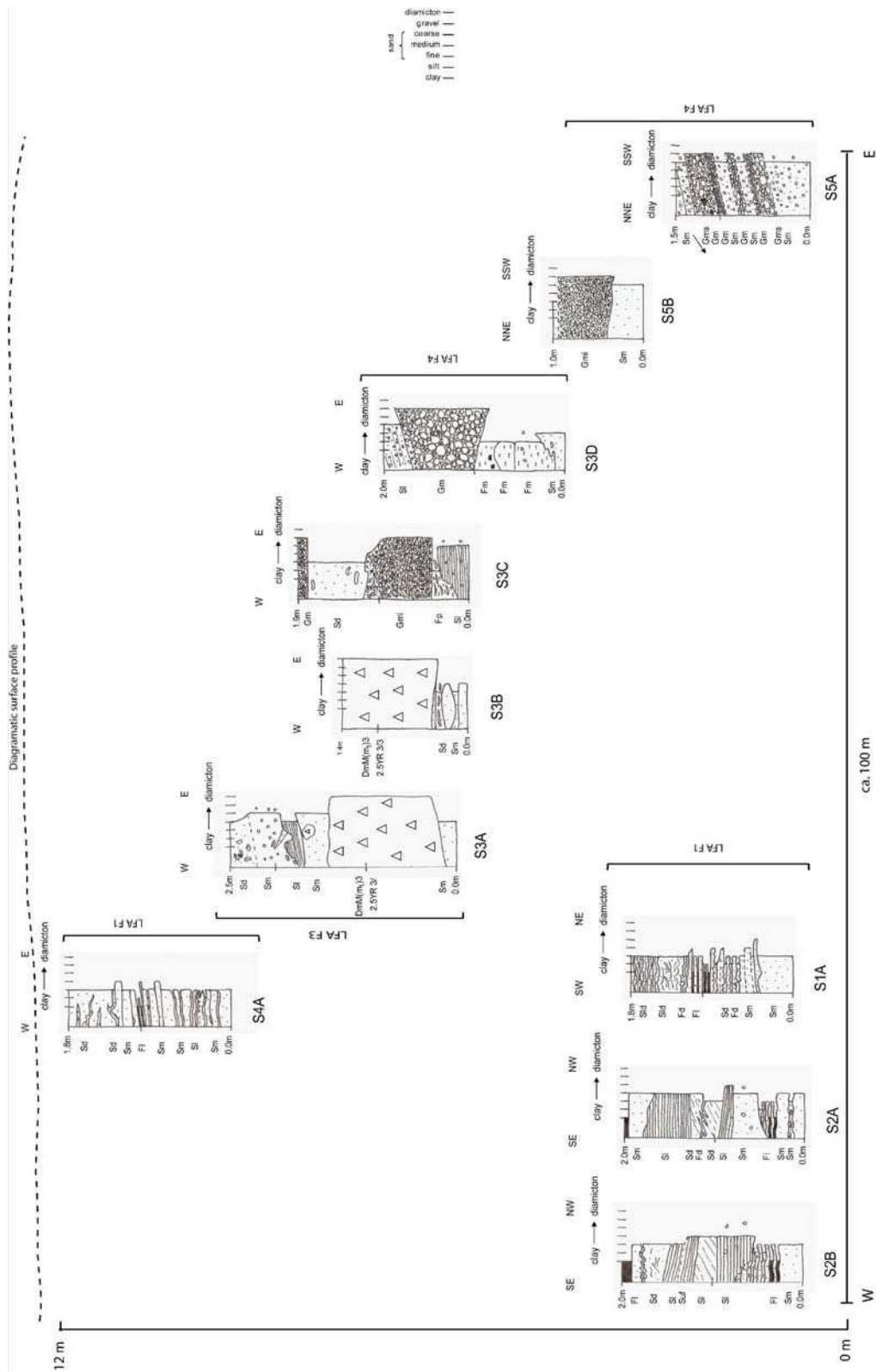*Figure 13:* Stratigraphic logs: Faugh sand pit

Figure 14: Photographs from faugh sand pit: (a) LFA F3: interdigited diamicton, massive sand and cross-bedded stratified sand and granule gravel; (b) LFA F3: sheared, incorporated lower boundary of the diamicton; (c) LFA F1: shallow dipping fine sand and thick fine-grained bands; (d) LFA F4: interbedded, clast supported granule-pebble gravel and stratified coarse sand with some gravel, massive coarse sand and wide, thin imbricated gravel lithofacies; (e) LFA F1: alternations of fine sand laminations and ripples structures; and (f) LFA F4: heavily faulted laminated sand and massive gravel lithofacies
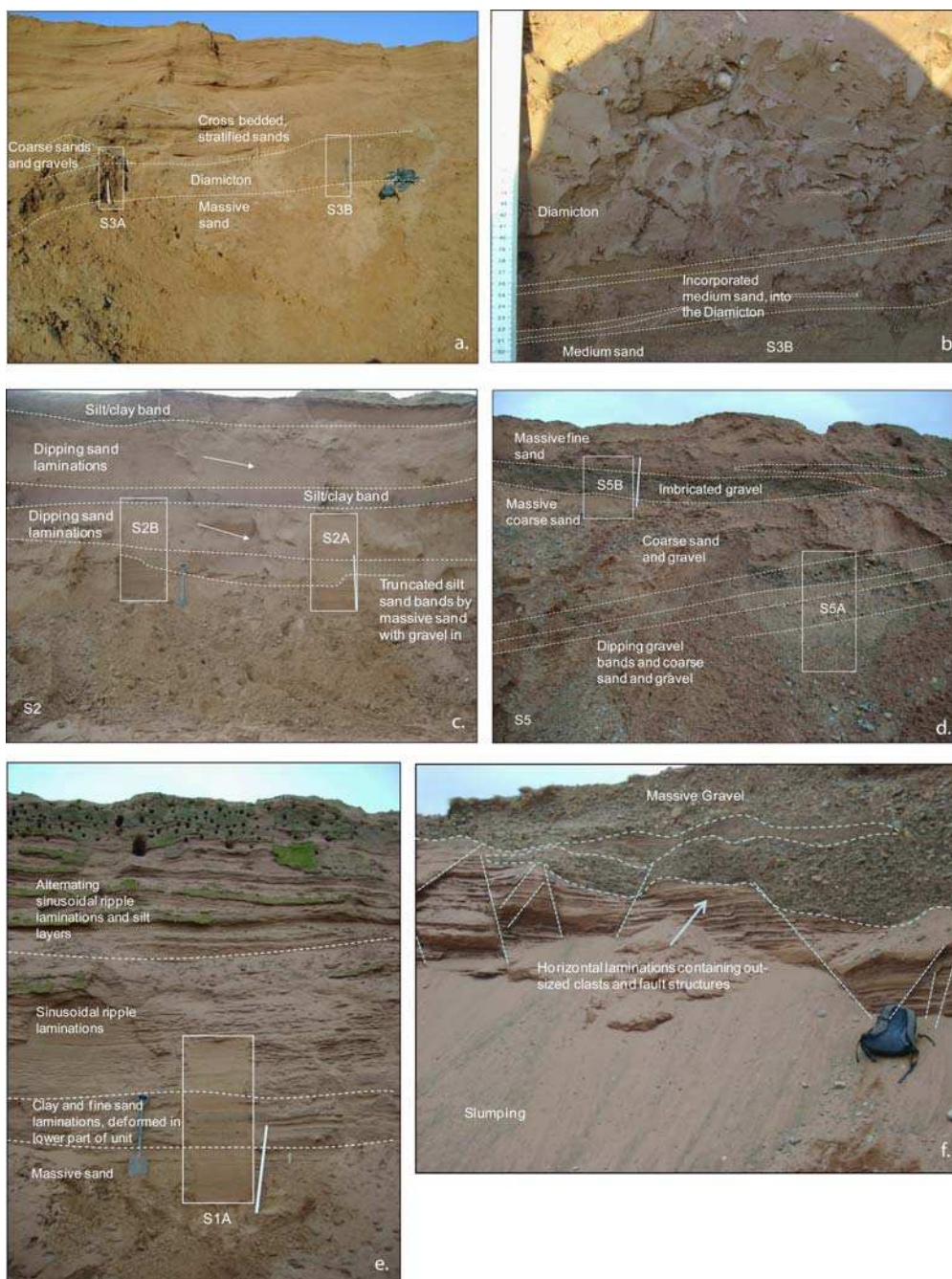
Figure 15: Modern Analogues (Iceland): (a) aerial photograph (2007) of Sandsfellsjökull (top-left) and its forefield, revealing a number of lakes; (b) ice-cored eskers and pitted outwash: Sandsfellsjökull; (c) pitted outwash: Bruarjökull; (d) glacier ice revealed beneath pitted outwash: Bruarjökull; (e) outwash covering the snout of Fjalljökull; and (f) ice-cored outwash fan and eskers at Fjalljökull.

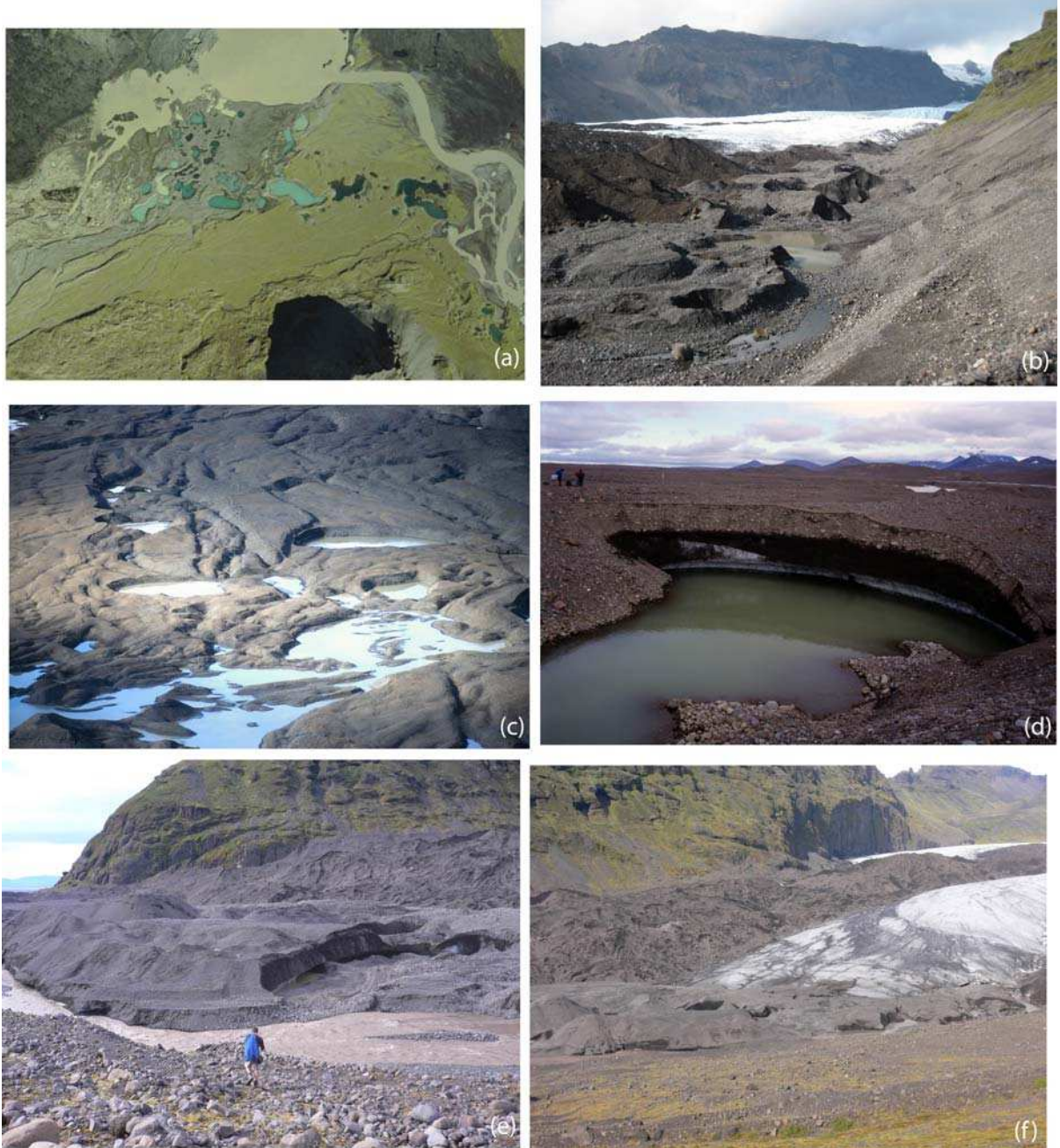*Figure 16:* Model of formation of the Brampton kame belt (based on the model by Brodzikowski & van Loon, 1991).